Marine Pollution Bulletin 197 (2023) 115746

Contents lists available at ScienceDirect

Marine Pollution Bulletin

journal homepage: www.elsevier.com/locate/marpolbul

Review

# Marine plastic pollution detection and identification by using remote sensing-meta analysis

Muhammad Waqas [a], Man Sing Wong [a,b,*], Alessandro Stocchino [c], Sawaid Abbas [d], Sidrah Hafeez [a], Rui Zhu [a,b]

[a] Department of Land Surveying and Geo-Informatics, The Hong Kong Polytechnic University, Kowloon, Hong Kong, China
[b] Research Institute of Land and Space, The Hong Kong Polytechnic University, Kowloon, Hong Kong, China
[c] Department of Civil and Environmental Engineering, The Hong Kong Polytechnic University, Kowloon, Hong Kong, China
[d] Remote Sensing, GIS and Climatic Research Lab (RSGCRL), National Center of GIS and Space Applications, University of the Punjab, Lahore 54590, Pakistan

ARTICLE INFO

*Keywords:*
Remote sensing
Floating plastic
Marine debris
Plastic detection

ABSTRACT

The persistent plastic litter, originating from different sources and transported from rivers to oceans, has posed serious biological, ecological, and chemical effects on the marine ecosystem, and is considered a global issue. In the past decade, many studies have identified, monitored, and tracked marine plastic debris in coastal and open ocean areas using remote sensing technologies. Compared to traditional surveying methods, high-resolution (spatial and temporal) multispectral or hyperspectral remote sensing data have been substantially used to monitor floating marine macro litter (FMML). In this systematic review, we present an overview of remote sensing data and techniques for detecting FMML, as well as their challenges and opportunities. We reviewed the studies based on different sensors and platforms, spatial and spectral resolution, ground sampling data, plastic detection methods, and accuracy obtained in detecting marine litter. In addition, this study elaborates the usefulness of high-resolution remote sensing data in Visible (VIS), Near-infrared (NIR), and Short-Wave InfraRed (SWIR) range, along with spectral signatures of plastic, in-situ samples, and spectral indices for automatic detection of FMML. Moreover, the Thermal Infrared (TIR), Synthetic aperture radar (SAR), and Light Detection and Ranging (LiDAR) data were introduced and these were demonstrated that could be used as a supplement dataset for the identification and quantification of FMML.

## 1. Introduction

Marine debris, also known as marine pollution, refers to solid materials, such as plastic bottles, fishnets, bags, etc., intentionally or unintentionally disposed into the ocean (Martínez-Vicente et al., 2019; Sojobi and Zayed, 2022; Walker et al., 2006). In the past three decades, plastic production has increased drastically due to population growth and economic development (Balsi et al., 2021; Borrelle et al., 2020; Lebreton et al., 2017; Sakti et al., 2021), and its significant portion was disposed into the ocean (Gall and Thompson, 2015; Ramavaram et al., 2018; Thompson et al., 2004). Low-cost single-use plastic, i.e., for packaging, is a significant source of plastic waste (Phillips et al., 2020; Prata et al., 2019). The recent COVID-19 pandemic has increased the demand for single-use plastic and intensified the already uncontrollable plastic pollution problems (Rakib et al., 2021). Plastic pollution in the ocean is primarily due to the mismanagement of plastic waste in the terrestrial environment (Abreu and Pedrotti, 2019; Jambeck et al., 2015; Law et al., 2010). Human and industrial waste is dumped into the ocean in developing countries (Phelan et al., 2020; Thompson et al., 2004; Walker et al., 2006), including micro and macro plastic (Woodall et al., 2014). Moreover, rivers transport plastic waste from land to the ocean (Lebreton et al., 2017; Meijer et al., 2021). Approximately 8 million metric tons of plastic pollute the ocean from land yearly (Jambeck et al., 2015; Worm et al., 2017), and about 80 % of the total ocean pollution consists of plastic litter (Abreu and Pedrotti, 2019; Almroth and Eggert, 2019; Meijer et al., 2021; Themistocleous et al., 2020). Under the current global production and usage statistics, it is estimated that the amount of plastic polluting the marine environment could nearly triple, from 14 million tons per year in 2016 to a projected 23–37 million tons per year in the next two decades (Borrelle et al., 2020; Kanhai et al., 2022; Lins-Silva et al., 2021; Marshall, 2018). Plastics accumulate in the marine environment, can travel thousands of kilometre, and persist for

* Corresponding author at: Department of Land Surveying and Geo-Informatics, The Hong Kong Polytechnic University, Kowloon, Hong Kong, China.
*E-mail address:* Ls.charles@polyu.edu.hk (M.S. Wong).

https://doi.org/10.1016/j.marpolbul.2023.115746
Received 15 February 2023; Received in revised form 30 October 2023; Accepted 31 October 2023
Available online 9 November 2023

decades (Lebreton et al., 2017; Sobhytta et al., 2020), thus creating significant adverse impact on the marine environment (Cole et al., 2011; Cózar et al., 2021; Walker et al., 2006).

Persistent plastic pollution adversely impacts aquatic life and becomes a major global environmental challenge (Chitrakar et al., 2019; Lebreton et al., 2018; Worm et al., 2017). Both marine and terrestrial ecosystems are linked (Bradney et al., 2019; Dang et al., 2022). Plastic pollution in the marine ecosystem poses a significant threat to marine animals, megafauna species, and planktonic microorganisms (Brandon et al., 2020; Wilcox et al., 2015). For endangered species such as marine mammals, sea birds, marine turtles, and fishes, its chemical and physical properties cause entanglement and blockages in the digestive tract, which leads to false satiation (Abreo et al., 2023; Schuyler et al., 2016) (Fig. 1). The chemical impacts of ingested micro and macro plastic by fishes are also a growing concern for human health (Dang et al., 2022; Gall and Thompson, 2015; Peng et al., 2020; Zhang et al., 2020). The plastic's chemical compounds may bioaccumulate into the human food chain and its implications, making it a human health hazard (Dang et al., 2022; Schmaltz et al., 2020). When these wash ashore, it can also cause negative impacts on socio-economic and tourism activities on the shore (Alosairi et al., 2021; Cecchi, 2021).

In light of the growing concerns about the negative impacts of plastic pollution on the marine environment, various governments and international governing bodies are increasingly mitigating this global issue (Adam et al., 2020). From 1991 to now, more than 36 policies have been established that aim at reducing single-use plastic (Kanhai et al., 2022; Schmaltz et al., 2020). The United Nations Environment Assembly (UNEA) has also passed many resolutions to reduce marine plastic pollution and acknowledged marine plastic pollution as one of the intensified global challenges affecting the marine ecosystem associated with human health and coastal economic assets (Cecchi, 2021; Dang et al., 2022; OHHLEP et al., 2022; Schmaltz et al., 2020; Xanthos and Walker, 2017). Due to its global concern, the United Nations Environment Program (UNEP) identified marine plastic pollution as an emerging global environmental problem (Marshall, 2018; Mouat et al., 2010) and estimated that about US$ 13–19 billion per annum damages to the marine ecosystems (Viool et al., 2019). Thus, the identification and detection of plastic pollution in the ocean align with the United Nations (UN) Sustainable Development Goals (SDGs) for 2030, especially Goal 14 (Life Below Water), which is directly linked to Goal 15 (Life on Land), Goal 12 (Responsible Consumption and Production), Goal 11 (Sustainable Cities and Communities) and Goal 17 (Partnership for Goals) (UN, 2016).

### 1.1. *Remote sensing of marine litter*

Remote sensing data has proved its potential and usability in monitoring environmental issues. In the past decade, remote sensing data has been used to identify, quantify, and detect plastic litter in the terrestrial and marine environment (Fig. 1). For example, remote sensing data is used to quantify agricultural plastic waste (Lanorte et al., 2017; Sakti et al., 2021; Zhang et al., 2022), terrestrial aggregated plastic waste (Kruse et al., 2023; Page et al., 2020) and marine plastic litter (Mace, 2012; Taggio et al., 2022; Vitale et al., 2022). Novelli and Tarantino (2015) used the spectral band to separate the plastic litter from vegetation, sand, and water in the terrestrial environment using the Landsat

**Fig. 1.** Remote Sensing of floating marine plastic pollution in marine environment.

8 OLI/TIRS spectral bands. Goncalves et al. (2020) used high-resolution aerial photographs for mapping plastic litter on Cabedelo beach dune systems. Another study by Acuna-Ruz et al. (2018) assessed the spectral characterization of marine debris on beaches and quantified litter amounts using the automatic digital classification of very high-resolution aerial imagery. Similarly, Hu (2021) assessed the spectral characteristics of different bands of moderate spatial resolution Sentinel-2 satellite data in the visible (VIS) and near-infrared (NIR) spectra, for detection and differentiation of various forms of plastic debris in the marine environment. Sasaki et al. (2022) used very high-resolution Worldview 2/3 satellite data to map the marine debris concentration and distribution along the southern island of Japan. Goddijn-Murphy et al. (2022) explored the potential use of thermal infrared (TIR) sensor data, complimenting VIS, NIR, and SWIR sensors and demonstrating its effectiveness in distinguishing plastic litter at night time from other floating materials. Cocking et al. (2022) used the hyperspectral short-wave infrared (SWIR) sensor data to detect marine plastics in a sandy shoreline environment. Different methods were developed to monitor micro and macro plastic debris polluting coastal environments which demonstrated the potential use of active and passive remote sensing data (Ge et al., 2016; Guffogg et al., 2021; Mukonza and Chiang, 2022; Ormaza-Gonzaìlez et al., 2021; Taddia et al., 2021; Veettil et al., 2022; Yuying et al., 2019). Further research explored the marine debris accumulating in the coastal environment either washed ashore during extreme oceanic events or dumped intentionally (Aoyama, 2016; Arii et al., 2012; Hu et al., 2023; Nakajima et al., 2022). These studies demonstrated the potential use of remote sensing data for plastic floating in the marine environment.

Therefore, long-term or short-term monitoring of floating marine macro litter (FMML) should be well studied. Different methods to detect, classify, quantify, and track FMML, primarily using multi-source remote sensing data, including visual interpretation (Garcia-Garin et al., 2020a, 2020b; Kikaki et al., 2020; Konstantinos Topouzelis et al., 2019), spectral reflectance interpretation (Ciappa, 2022; Goddijn-Murphy and Dufaur, 2018; Hu, 2022, 2021; Hueni and Bertschi, 2020; Moshtaghi et al., 2021; Papageorgiou et al., 2022; Tasseron et al., 2021), modelling (Dasgupta et al., 2022; Kikaki et al., 2020; Lebreton et al., 2018; Sebille et al., 2020) and image-based classification (Basu et al., 2021; Biermann et al., 2020; de Vries et al., 2021; Freitas et al., 2022; Garcia-Garin et al., 2021; Jamali and Mahdianpari, 2021; Kikaki et al., 2022; Kremezi et al., 2021; Mifdal et al., 2021; Olyaei et al., 2022). Multi-source remote sensing sensor data used in VIS, NIR, and SWIR spectral range includes multispectral and hyperspectral cameras (Balsi et al., 2021; Garaba et al., 2021; Garaba and Dierssen, 2018; Garcia-Garin et al., 2021; Wolf et al., 2020), spectral radiometry (Goddijn-Murphy and Dufaur, 2018; Moshtaghi et al., 2021; Tasseron et al., 2021) and satellites imagery (Hu et al., 2022; Kikaki et al., 2022; Kremezi et al., 2022, 2021; Mifdal et al., 2021; Park et al., 2021; Taggio et al., 2022), complemented by TIR imaging (Goddijn-Murphy et al., 2022; Goddijn-Murphy and Williamson, 2019), Synthetic aperture radar (SAR) (Aoki et al., 2013; Simpson et al., 2022; Topouzelis et al., 2019), microwave X-band radar (Serafino and Bianco, 2021; Simpson et al., 2023), Light Detection and Ranging (LiDAR) (Feygels et al., 2017; Lebreton et al., 2018; Mace, 2012), video imaging techniques (Armitage et al., 2022; de Vries et al., 2021; Teng et al., 2022). Many governmental agencies, environmental groups, and the research community have started to collaborate and develop integrated FMML detection methods using multi-source remote sensing data due to their greater synoptic and frequent coverage (Andriolo et al., 2020; Garaba et al., 2018; Maximenko et al., 2019; Vighi et al., 2022). Optical sensors installed on satellites, aircraft, drones, and handheld devices mounted on vessels, along with the in-situ spatial and temporal data, can contribute to the identification of FMML effectively (de Vries et al., 2021; Martínez-Vicente et al., 2019; Moshtaghi et al., 2021; Serafino and Bianco, 2021). Satellites with moderate spatial resolution (Sentinel-2 A/B) to high resolution (Worldview 2, 3 and PlanetScope) can readily identify and detect the shape and size of FMML (Biermann et al., 2020; Kikaki et al., 2022; Kremezi et al., 2022; Sannigrahi et al., 2022), while volume and distribution of the large patches FMML could be precisely quantified by SAR (Davaasuren et al., 2018; Simpson et al., 2022; Konstantinos Topouzelis et al., 2019) and LiDAR (Feygels et al., 2017; Lebreton et al., 2018; Pichel et al., 2012). The recent development in the multispectral and hyperspectral remote sensing data enabled us to detect the spectral reflectance of moving plastic in the ocean using the VIS, NIR, and SWIR wavelengths (Garaba and Dierssen, 2020; Mehrubeoglu et al., 2020; Schmidt et al., 2018; Verstraete et al., 2015). The satellite with a hyperspectral sensor (PRISMA) can detect the FMML using the spectral values of plastic materials (Goddijn-Murphy and Dufaur, 2018; Serranti et al., 2019); however, the spatial resolution of the satellite sensor shall be high enough to capture the size and shape of FMML (Kremezi et al., 2021; Maximenko et al., 2019; Park et al., 2021). The researcher utilized the spectral signature of plastic for carefully selecting the spectral band to develop different spectral indices for identifying FMML. Additionally, they used different artificial plastic targets to increase the accuracy of the developed spectral index. They have used in-situ data and the results from spectral indices to train different supervised and unsupervised image classification methods (Gnann et al., 2022; Maximenko et al., 2019; Mukonza and Chiang, 2022). Recent studies showed that FMML >2.5 cm can be identified using high-resolution aerial imagery using highly trained models and developed methods (Goddijn-Murphy and Dufaur, 2018; Hanvey et al., 2017; Kremezi et al., 2022; Wolf et al., 2020).

Due to increased concern related to the monitoring of FMML, the researcher reviewed the method employed and data used, as well as discussed the gaps and limitations between them. Initially, Veenstra and Churnside (2012) outlined that many airborne sensors (active and passive) could be used to detect marine plastic from a theoretical standpoint. Similarly, Mace (2012) reviewed marine debris monitoring technologies, methods, and issues, focusing on improving the Ghost Net Project, which pioneered the integration of models, satellite observations, and aircraft surveys for debris tracking. Similarly, Martínez-Vicente et al. (2019) published an early assessment of the primary process requirement, spectrally and spatially, relevant to marine plastic pollution monitoring by using remote sensing data, as well as a description of existing methods with the potential for detecting FMML. Similarly, Maximenko et al. (2019) proposed an integrated marine debris observing system (IMDOS) that combines optical remote sensing sensor data (Multi-hyper spectral) and in-situ data to maximize the efficiency of long-term monitoring of anthropogenic pollution in coastal ecosystems. Another review by El Mahrad et al. (2020) identified how different remote sensing data technologies can fill the gaps in monitoring multiple coastal and environmental issues, including plastic litter. Farré (2020) compared the applicability of various data collection approaches to detect marine contaminants of emerging concern (CECs) and plastic litter. Recently, Schmid et al. (2021b) reviewed the method and data used for assessing the presence of micro and macro plastic in the water, beach, seabed, and aquatic life of the marine ecosystem of the Adriatic region. Similarly, Salgado-Hernanz et al. (2021) reviewed all techniques used to detect plastic litter (micro and macro) and Sea-slicks using all types of sensors in the ocean water and beaches comprehensively. Topouzelis et al. (2021) conducted a comparable review on the use of satellite data to detect plastic on land, beaches, in-land water bodies, and the ocean. Mukonza and Chiang (2022) follow a similar approach to provide a detailed bibliographic review of different methods to detect and quantify marine litter using satellite-based remote sensing data. Vighi et al. (2022) provided an overview of the recent developments and trends in different methodologies used for FMML detection. Another comparable review by Veettil et al. (2022) evaluated the merits and limitations of using different remote sensing data (platform and sensors) for detecting and controlling floating and beached marine plastic litter. Similarly, Gnann et al. (2022) conducted a review of studies that explored at the spectral and spatial characteristics

of imaging sensors, primarily employing machine learning to identify riverine and marine plastic litter. Recently, Yuan et al. (2023) discussed the challenges of using unmanned vehicular platforms (UVP) such as UAV, USV and vessels compared to satellite for detection and quantification of marine environment monitoring (biochemical, physical, pollution, aerosols). All of these reviews had a similar objective and approach for examining the literature about detecting, quantifying, classifying and tracking marine litter, highlighting the trends in multi-source remote sensing techniques. Therefore, in this review, we aim to summarize the most recent developments and trends in methods and data used, primarily for the identification and detection of FMML in the ocean, and to discuss how a methodological frameworks could be developed in future using optimal data and methods used for FMML detection (Fig. 1). The objective of this systematic assessment includes: i) evaluation and identification of the most suitable remote sensing platforms and sensors to detect FMML in open and coastal ocean water, ii) the most applicable and optimal spatial and spectral resolution ranges, and iii) evaluation of the accuracy obtained for the methods used for FMML detection.

## 2. Methodology

### 2.1. Search strategy

To conduct a systematic review and meta-analysis according to the Preferred Reporting Items for Systematic reviews and Meta-Analysis (PRISMA) guidelines, we first undertook bibliographic research on various scientific publications. To this end, a specific research topic was selected, namely "detection and identification of floating marine macro plastic litter using remote sensing". The studies focused on floating marine plastic pollution detection using remote sensing techniques, published between January 1, 2010 and August 31, 2023, and indexed in two English databases (Web of Science and Scopus) were identified. Our search strategies were based on the combinations of "Marine Plastic Pollution" and "Remote Sensing" terms. The detailed search strategy is shown (Table 1). We excluded the review papers, book chapters, and reports during the literature search to find the eligible studies. Then, the eligible research studies with title, abstract, DOI, and journal names were exported from the databases.

**Table 1**
Key word search for literature search in two databases (Scopus & Web of Science).

| Database | Search strategy | Results |
|---|---|---|
| Scopus | (TITLE-ABS-KEY (marine OR ocean OR sea) AND TITLE-ABS-KEY (plastic* OR malleable OR pliable OR ductile OR flexible OR workable OR moldable) AND TITLE-ABS-KEY (pollut* OR contaminat* OR litter OR waste OR debris OR scrap) AND TITLE-ABS-KEY ((remote* AND sens*) OR (remot* AND sens*) OR airborne OR satellite OR UAV OR lidar OR sar OR optical OR (aerial AND photo) OR drone OR USV) AND TITLE-ABS-KEY (detect* OR discrimin* OR assess* OR monitor* OR observ* OR analys* OR find* OR identif* OR map* OR classif*)) AND PUBYEAR >2009 AND (EXCLUDE (DOCTYPE, "re") OR EXCLUDE (DOCTYPE, "cr")) | 421 |
| Web of Science | marine OR ocean OR sea (All Fields) and plastic* OR malleable OR pliable OR ductile OR flexible OR workable OR moldable (All Fields) and pollut* OR contaminat* OR litter OR waste OR debris OR scrap (All Fields) and (remote* AND sens*) OR (remot* AND sens*) OR airborne OR satellite OR UAV OR lidar OR SAR OR optical OR (aerial AND photo) OR drone OR usv (All Fields) and detect* OR discrimin* OR assess* OR monitor* OR observ* OR analys* OR find* OR identif* OR map* OR classif* (All Fields) and Review Articles (Exclude – Document Types) | 453 |

### 2.2. Selection criteria

A double screening method was adopted to reduce the screening biasness and to resolve any conflict in the inclusion and exclusion of research studies. The screening, inclusion, and exclusion were done within an online platform, Covidence.org, which is helpful for systematic review and meta-analysis workflow. After obtaining eligible studies from the literature search, we imported 874 total references into Covidence. After removing 223 duplicates from the literature, two authors independently screened titles and abstracts according to the searched keywords (Fig. 2). If a conflict arose, it was resolved in the full-text screening. After the title and abstract screening process, both authors prioritized the inclusion of the literature in the full-text screening process. During the full-text screening process, priority was given to those studies that used remote sensing data to identify floating macro marine litter, reported the accuracy of the method used, and the detected plastic target sizes if deployed or targeted as a pre-defined outcome of the study. Based on our designed criteria, we found the major exclusion criteria such as wrong setting, wrong study objectives, wrong study area, wrong data used, wrong method used, and wrong outcomes during the full-text screening of the studies (Fig. 2). The wrong setting is referred to as lab-based or experimental studies conducted in a controlled environment, while the wrong study objective criteria are referred to as the study objectives not inclined with our research question. Similarly, the wrong study area includes the beaches, riverine water, estuarine water, wetlands, and terrestrial regions, while the wrong data used referred to fishnet trawls, quantitative surveys, water sampling, laboratory experiments, etc. Furthermore, the wrong method used and wrong outcome criteria are referred to as not inclined with our research question. After the initial and full-text screening, we found 48 eligible studies for systematic review and meta-analysis.

### 2.3. Data extraction

Two authors independently extracted the following information from the included studies using Covidence. The extracted information includes Title, Author name, Abstract, Published Year, Journal name, DOI, Citation, Country of Study, Aim of the Study, Study Design, Study Area, Water Body, Spatial Coverage, Temporal Coverage, Date of Data Acquisition, Platform, Sensor, Height of Platform, Imaging Mode, Band Used, Indices Used, Spectral Range, Spatial Resolution, In-Situ data, Ancillary Data, Wind Speed, Overall Oceanic Condition, Inclusion Criteria, Plastic Detection Method, Largest Detected Plastic Target, Smallest Detected Plastic Target and Total Accuracy obtained in the detection of FMML (Table 2). If any conflict was found in the information extracted from both authors, it was resolved with the help of a third author.

### 2.4. Quality assessment

After data extraction, we assessed eligible studies based on different assessment domains such as data used, method used, and accuracy of the method for detecting and identifying FMML. In the quality assessment, each author gives a score (very high quality, high quality, moderate quality, and low quality) after assessing each eligible study based on defined key criteria for each domain, such as data used, method used, and accuracy (Table A1). The third author would resolve the conflict if there were any. We included only those studies in our systematic review that fulfilled the selection criteria and contributed to method developments for the FMML detection. After the quality assessment, we further removed 4 studies during the data extraction and included the 44 studies for the review.

### 2.5. Risk of biasness assessment

We have assessed the risk of biasness for each included eligible study

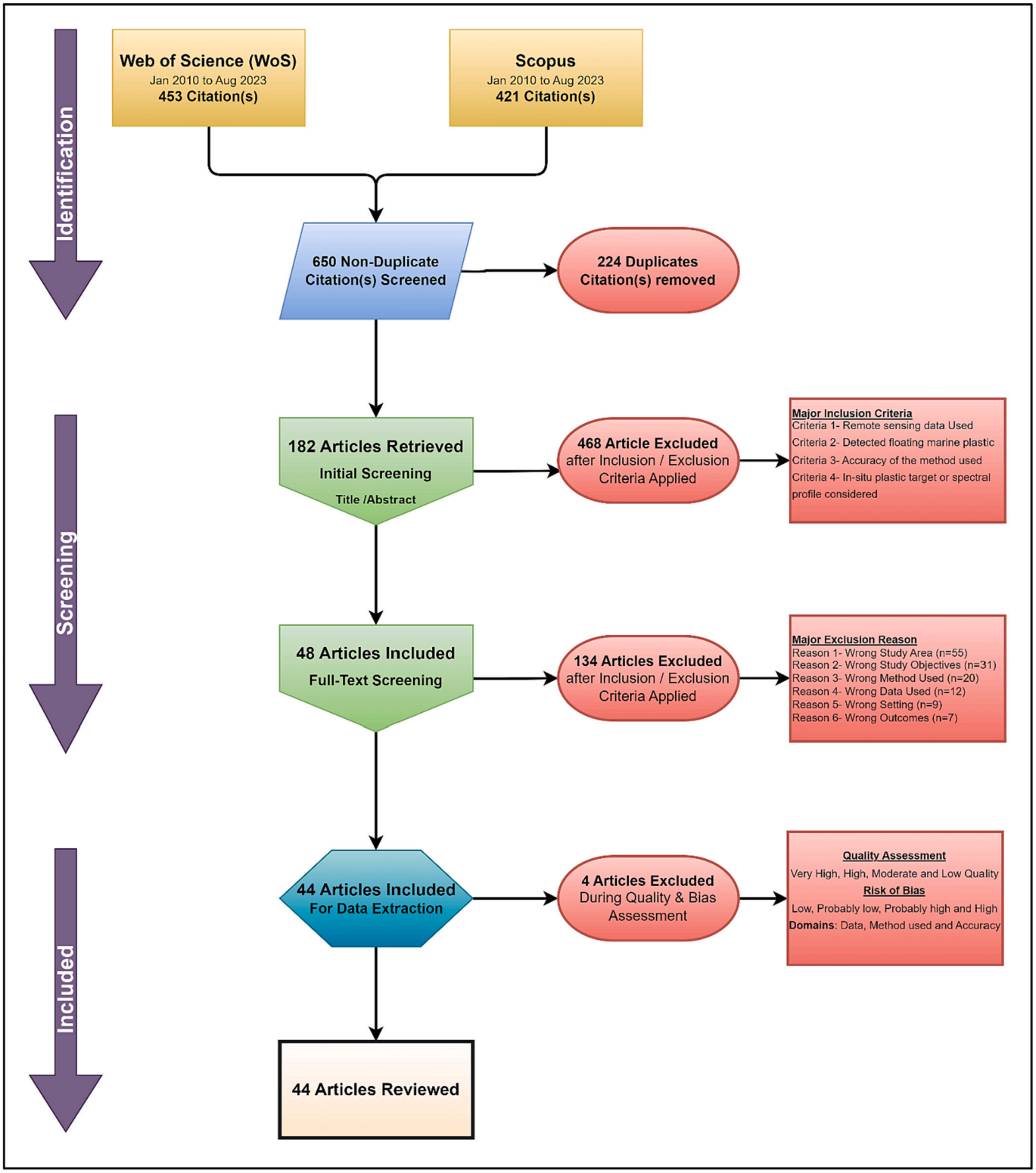


**Fig. 2.** Preferred Reporting Items for Systematic reviews and Meta-Analysis (PRISMA), Inclusion/Exclusion criteria for quality assessment and risk of biasness.

for the meta-analysis which is different from the methodological quality assessment of the selected research studies. There are many risks of biasness assessment methods for different research domains but to our best knowledge, no validated tools are currently available to assess this risk. Thus, to avoid any risk of biasness in the selection of studies, two authors assessed the risk of biasness in the selection process for eligible studies according to the well-defined key parameters based on the inclusion and exclusion criteria of the studies. The risk of biasness was assessed and given a score from low risk of biasness, probably low risk of biasness, probably high risk of biasness or high risk of biasness according to the fulfilment of the pre-defined key criteria's (Table A1).

**Table 2**
Data extraction parameters of each study included.

| General parameters | Key parameters |
|---|---|
| General information | Title; Authors; Abstract; Published Year; Journal; DOI; Citation and Country of Study |
| Characteristics of the study included | Aim of the Study; Study Design; Study Area; Water Body; Spatial Coverage; Temporal Coverage |
| Data used | Date of Data Acquisition; Platform; Sensor; Height of Platform; Imaging Mode; Band Used; Spectral Range; Spatial Resolution; In-Situ Data; Ancillary Data; Wind Speed and Overall Oceanic Condition |
| Method used | Plastic Detection Method; Indices Used; Largest Detected Plastic Target; Smallest Detected Plastic Target and Total Accuracy |

## 3. Results

Studies found by following the literature search were categorized based on key characteristic parameters such as remote sensing platform, sensor, spectral resolution, study area, spatial resolution, indices, detected plastic target and methodology for marine litter classification and detection. Due to the diversity in data and methods used to detect marine plastic litter, these key parameters help us understand the accessibility and useability of using remote sensing data for the assessment.

### 3.1. Data used

#### 3.1.1. Remote sensing data

The remote sensing platform has been categorized into 3 types: spaceborne, airborne (aerial or drones), and ground-based or lab-based. Different types of active and passive sensors are mounted on these platforms, which collect information about the Earth's environment. In the selected studies, the platforms used in the remote sensing data acquisition, such as satellite remote sensing, aerial remote sensing or manned aircraft, unmanned aerial vehicle, the static sensor on the ground, and mounted on fixed-view cameras.

From the bibliographic review (Table 3), around 50 % of the included studies used only spaceborne platforms for remote sensing sensors including Sentinel-1/2 A/B, PRISMA, PlanetScope, Worldview 2,3, TIR, MODIS, RADARSAT-1, and Landsat 8 OLI sensor (Biermann et al., 2020; Booth et al., 2023; Goddijn-Murphy and Williamson, 2019; Hu et al., 2023; Kremezi et al., 2021; Mifdal et al., 2021; Papageorgiou et al., 2022; Park et al., 2021; Simpson et al., 2022; Konstantinos Topouzelis et al., 2019). Similarly, about 23 % of studies have used only airborne sensor multispectral and hyperspectral data (VIS, NIR, and SWIR, and LiDAR sensors) (Almeida et al., 2023; Balsi et al., 2021; Feygels et al., 2017; Freitas et al., 2022; Garcia-Garin et al., 2021; Hueni and Bertschi, 2020; Lebreton et al., 2018; Wolf et al., 2020) and around 9 % used both spaceborne and airborne sensor data (Gonzaga et al., 2021; Pichel et al., 2012; Themistocleous et al., 2020; Topouzelis et al., 2020b). Similarly, around 9 % used a controlled environment or lab-based platform for remote sensing sensors. The lab-based controlled environment evaluated the spectral signatures of plastic materials for the selection of satellite spectral bands (Moshtaghi et al., 2021; Tasseron et al., 2021) or the development of FMML identification models (Goddijn-Murphy and Dufaur, 2018). Similarly, 7 % of the studies used vessel-based photos or videos for the identification of plastic in the ocean at different times and spaces (Armitage et al., 2022; de Vries et al., 2021) with the help of airborne data (Garcia-Garin et al., 2020b). Only one unique study has employed an X-band radar mounted on a building to track the trajectory of FMML by utilizing the reflective intensity of the targeted materials (Serafino and Bianco, 2021). It is also worth noting that the Sentinel-2 sensor has been widely used along with other remote sensing data due to its sufficient spatio-temporal resolution for detecting floating marine litter (Hu, 2022) (Table 3).

#### 3.1.2. In-situ data

In-situ data is required to integrate with remote sensing data to supplement the remote sensing observation of the earth's environment. The purpose of in-situ data is to supplement the remote sensing-based plastic identification methods and models (Biermann et al., 2020). From the bibliographic review of the literature, in-situ data were collected by evaluating the spectral reflectance of plastic materials in the labs or deploying physical plastic targets in the ocean (Table 3). During the lab-based controlled experiments, plastic targets were made with different plastic materials (e.g., plastic drink bottles or carrier bags) placed in the sensors' field of view. Spectral profiles of different wet and try plastic targets were developed using the spectrometer detection method and considered as reference data for the FMML identification methods (Goddijn-Murphy and Dufaur, 2018; Moshtaghi et al., 2021; Tasseron et al., 2021). Similarly, different plastic targets were deployed in the ocean at a specified time and space to collect the overpassing satellite data for training the image classification methods. Topouzelis et al. (2019) deployed a plastic target of 10 × 10 m, and similarly, Topouzelis et al. (2020a) deployed different targets of 5 × 5 m, 5 × 10 m, 10 × 10 m, and 5 × 20 m sizes into the Aegean sea at different time and space. Similarly, Kremezi et al. (2021) used 0.6 m × 0.6 m and 2.4 m × 2.4 m smaller targets, and 5.1 m × 5.1 m targets equal to image resolution along the Lesvos island, Greece, and Jamali and Mahdianpari (2021) used comparatively larger targets of sizes (45 m × 5 m, 21 m × 10 m) in Mytilene, Greece. Kikaki et al. (2022) compiled a standard dataset, Marine Debris Archive (MARIDA), to develop and evaluate machine learning models for marine debris detection by distinguishing them from other floating materials. Some other studies use plastic targets from projects, such as Plastic Litter Project 2018 2019, 2020, 2021, 2022 (Papageorgiou et al., 2022; PLP, 2023; Topouzelis et al., 2019; Topouzelis et al., 2020a) and Marine Debris Archive (MARIDA) (Kikaki et al., 2022), to develop and train their plastic detection methods in the marine environment (Table 3).

### 3.2. Spatial resolution

In a remote sensing system, spatial resolution refers to pixel size and the ability of the sensor to outline and depict the characteristics of particular earth features (Omali, 2018; Waqas et al., 2019). Recent developments in high-resolution satellite imagery, FMML ≤5 m can be identified by employing different spectral indices and image classification methods. All the eligible studies have used remote sensors with moderate to high spatial resolution satellite imagery such as Landsat 8 (30 m), Sentinel-2 (10 m for VIS and NIR and 20 m for SWIR bands), PRISMA (30 m and 5 m pan band), PlanetScope (3 m), Worldview-2/3 (1.84 m, 1.2 m), and very low-resolution data from MODIS Aqua/Terra (250 m) etc. (Table 3). Similarly, aerial photography using RGB and hyperspectral SWIR cameras mounted on UAVs and aircraft has a higher spatial resolution from 0.10 cm to 5 cm due to low flight height. Specifically, vessel-based (across-track) image expedition can easily detect a plastic target >2 cm. We observed that 11 studies have used Sentinel-2 A/B data despite having a moderate spatial resolution of 10 m along with other high-resolution satellites and aerial imageries (Table 3). The Sentinel-2 satellite has a clear advantage of its unique spectral band in VIS, NIR, and SWIR region and large synoptic view. It is worth highlighting that upscaling image resolution by pan-sharpening algorithms can resample the Sentinel-2 (20 m and 60 m) bands to 10 m spatial resolution. Hu (2022) explained the useability of Sentinel-2 when detecting the floating marine litter in the ocean. Similarly, Kremezi et al. (2021) pan-sharpened the PRISMA hyperspectral imagery from 30 m to 5 m, and Park et al. (2021) pan-sharpened the Worldview of 1.2 m multispectral bands to 0.3 m spatial resolution. Similarly, Kremezi et al., 2022 used image fusion of Sentinel-2 images with high-resolution WorldView-2/3 images to detect the 0.6 m × 0.6 m plastic target. It is considered that high spatial resolution satellite data can detect FMML ≤1.5–3 $m^2$ in ideal conditions, and image fusion can

**Table 3**
Key parameters of the included study such as sensor used, spectral range, spatial resolution, in-situ data, indices used, image classification method, detected plastic target sizes and the accuracy of the method used.

| Reference | Sensor | Platform | Spectral range | Band used | Spatial resolution | In-Situ data | Indices used | Image classification | Largest detected plastic | Smallest detected target | Accuracy obtained |
|---|---|---|---|---|---|---|---|---|---|---|---|
| (Feygels et al., 2017) | Lidar, RGB camera and the integrated ITRES SASI SWIR sensor | Airborne | VIS, SWIR, LiDAR | RGB (465–630 nm) SWIR Imager (950–2450 nm) | 4800 by 3200-pixel resolution for RGB cam 30 × 30 microns for ITRES SASI SWIR imager | NA | NA | Image Fusion | 1.54 m2. | 0.61 m2 | NA |
| (Garaba et al., 2018) | ITRES SASI-600 Hyperspectral | ≠ | RGB and Hyperspectral SWIR | RGB 400760 nm; SWIR 950–2450 nm | SASI imager was 0.5 m across × 1.2 m along the track, 0.1 m × 0.1 m for the RGB camera. | NA | NA | Overlaying SASI image on RGB | 0.5 × 1.2 m | 0.025 m × 0.06 m | 118 out of 1595 targets were identified by overlapping |
| (Lebreton et al., 2018) | Lidar, SWIR imager, and RGB camera (CS-4800i) | ≠ | RGB | B (458–523 nm) G (543–578 nm) R (650–680 nm) | ~0.1 m resolution | trawl sampling | NA | Photointerpretation and Empirical Modelling | >50 cm | 10–50 cm | NA |
| (Wolf et al., 2020) | DJI 4 Phantom Pro 20 MP | ≠ | ≠ | ≠ | pixel resolution of 4864 × 3648 | NA | NA | APLASTIC-Q Supervised (I) plastic litter detector (PLD-CNN) (ii) plastic litter quantifier (PLQ-CNN). | NA | >2.5 cm | PLD-CNN 83 % PLQ-CNN 71 %. |
| (Hueni and Bertschi, 2020) | (APEX 2.55000) (AVIRIS-ng 44,500) | ≠ | VIS-IR Imaging Spectrometer | 1667 nm, 1728 nm, and 1788 nm | APEX 2.5 cm AVIRIS-ng 4 cm | 10 m × 10 m (3 targets) 5 %, 2.5 % and 1 % abundance | NA | Linear Spectral Unmixing | 10 m × 10 m 5 % abundance | 10 × 10 m 1 % abundance | 1 % - 5 % abundance samples were identified |
| (Garcia-Garin et al., 2020a) | Canon EOS REBEL SL1 (Partenavia P-68) | ≠ | RGB | B (458–523 nm) G (543–578 nm) R (650–680 nm) | 2.5 cm | NA | NA | Photointerpretation | NA | 30 cm | Target detected 97 from Images 208 observer-based survey |
| (Garcia-Garin et al., 2021) | (1) Drone) DJI Mavic Pro (RGB Cam FC220, (2) aircraft (Partenavia P- 68), RGB Canon EOS REBEL SL1 | ≠ | ≠ | ≠ | 0.6 and 3.6 cm/ pixel for drones imagery 2.5 and 3.3 cm/ pixel for aerial survey | Plastic Targets (35 positive Control) | NA | CNN Supervised | 94 cm × 53 cm | 12 cm × 7 cm | During training 0.90 Testing 0.85. |
| (Balsi et al., 2021) | DJI Matrice 600 drone Hyperspectral SWIR | ≠ | Hyperspectral SWIR | Band-1950–1030 nm Band-21,110–1230 nm Band-31,440–1590 nm | 256 × 320-pixel resolution | Ground-based hyperspectral photography | NA | Supervised Classification Multi Class Linear Discriminant Analysis | 20 cm × 20 cm | 4 × 5 cm | 0.7 to 0.8 True Positive Rates vs. False Positive Rates |
| (Freitas et al., 2022) | VIS-SWIR hyperspectral imaging system (Specim FX10e) (HySpex Mjolnir S-620) | ≠ | 64 bands in VIS-SWIR (Selected) | Specim 400–1000 nm HySpex 970–2500 nm | Specim 1024 spatial pixels HySpex 620 spatial pixels | 10 × 10 m | NA | RF, SVM and CNN3D | 10 × 10 m | NA | RF 98.71 %, SVM 97 % and CNN3D 84.84 % |

(*continued on next page*)

**Table 3** (*continued*)

| Reference | Sensor | Platform | Spectral range | Band used | Spatial resolution | In-Situ data | Indices used | Image classification | Largest detected plastic | Smallest detected target | Accuracy obtained |
|---|---|---|---|---|---|---|---|---|---|---|---|
| (Almeida et al., 2023) | DJI Phantom 2 Vision + DJI Mavic 2 PRO | ≠ | RGB | B (458–523 nm) G (543–578 nm) R (650–680 nm) | 5472 × 3648 pixel resolution | 28 objects of floating plastic | NA | Visual Inspection Color- and Pixel-Based Detection Analysis CNN Supervised | NA | NA | 77.62 % Precision for CNN model |
| (Garcia-Garin et al., 2020b) | Phantom 3 Pro (Vessel), DJI Mavic Pro (Drone) | Airborne and Vessel | RGB | B (458–523 nm) G (543–578 nm) R (650–680 nm) | 2 cm per pixel for drone survey | Observer and Vessel-based survey | NA | Photointerpretation | >20 cm | NA | 99 % of the detected floating objects were plastic particles |
| (de Vries et al., 2021) | GoPro® cameras | Vessel | ≠ | ≠ | 4000 by 3000 pixels resolution | Vassel based Photography | NA | Tensor Flow Object Detection (FRCNN and YOLOv5) | 3 m | 0.15 m | Can identify targets ≥50 cm |
| (Armitage et al., 2022) | Vicon Fixed Bullet camera | Vessel | ≠ | ≠ | pixel resolution of 2592 × 1520 | Plastic bags (60 × 50 cm) and bottles (35× 10 cm) | NA | YOLOv5 | NA | >1 cm | 95.2 % |
| (Goddijn-Murphy and Williamson, 2019) | European Centre for Medium-Range Weather Forecasts (ECMWF), ERA5 Thermal Infrared | Spaceborne | TIR | medium-wave infrared (MWIR) 3–5 nm, long-wave infrared (LWIR) 8–14 nm | 27 km × 27 km | SST data at a grid of 0.25 × 0.25 degree | NA | Temperature difference between plastic and water | NA | NA | NA |
| (Kikaki et al., 2020) | PlanetScope, Sentinel-2 and Landsat 8 | ≠ | VIS-NIR, SWIR | All bands for PS, L8 and S2 (excluding 9,10) | PS 5 m, S2 10 m L8 30 m | Social media and Citizen science | NA | Image interpretation | 0.154 km2 | 0.019 km2 | NA |
| (Biermann et al., 2020) | Sentinel-2 | ≠ | ≠ | Band 4,6,8,11,12 | (Band 4 and 8) 10 m. (Band 6, 11 and 12) 20 m | 5 m × 5 m, 5 m × 10 m, 10 m × 10 m, 5 m × 20 m sizes | FDI and NDVI | Supervised Naïve Bayes | 26 pixels | 22 pixels | 86 %. |
| (Mifdal et al., 2021) | Sentinel-2 | ≠ | ≠ | All bands of S2 (442.7–2202.4 nm) | (Band 2,3,4,8)10 m, Band (5,6,7,8 A,11 and 12) 20 m (Band 1,9,10) 60 m | Social Media | FDI and NDVI | SVM, RF, Naïve Bayes and CNN-U-Net | NA | NA | SVM; 58.82 RV; 58.83 Naïve Bayes; 60.81 CNN (U-Net); 84.28 |
| (Kremezi et al., 2021) | PRISMA Hyperspectral | ≠ | ≠ | 175 bands in 400–2500 nm (excluding the bands in 1350–1470 nm and 1800–1950 nm range) | 30 m, pan band 5 m, after pan-sharpening, 5-m spatial resolution | plastic targets; 5.1 m × 5.1 m 2.4 m × 2.4 m 0.6 m × 0.6 m | Used FDI, NDVI and HI | Spectral Index development using VNIR bands (492, 596, 719,781, and 951) nm | 5.1 m × 5.1 m | 2.4 m × 2.4 m | NA |
| (Basu et al., 2021) | Sentinel-2 A and Setinel-2 B | ≠ | ≠ | Band 2–4,6,8,11,12 | Band 4 and 8) 10 m. (Band 6, 11 and 12) 20 m | 3 × 10 m Limassol, Cyprus 10 m × 10 m, 21 m × 10 m and 45 m × 5 m Mytilene, Greece | NDVI and FDI | Supervised SVR & SFCM Unsupervised K means, and Fuzzy c means | 45 m × 5 m (covers 6 pixels) | 10 m × 10 m (covers 4 Pixels) | SVR-96.9–98.4 %, SFCM 35.7 and 64.3 % FCM 69.8 and 82.2 %, K-means 69.8 to 81.4 %. |

(*continued on next page*)

**Table 3** (*continued*)

| Reference | Sensor | Platform | Spectral range | Band used | Spatial resolution | In-Situ data | Indices used | Image classification | Largest detected plastic | Smallest detected target | Accuracy obtained |
|---|---|---|---|---|---|---|---|---|---|---|---|
| (Khetkeeree and Liangrocapart, 2021) | Sentinel-2 | ⸗ | ⸗ | Band 3–6, 8, 11,12 | 10 m for Band 3,4, 20 m for bands 6,8,11, 12 | 3 m × 10 m Limassol, Cyprus | NDVI, RNDVI, PI, NDWI, FDI, INDVI, MINDVI | Developed MINDVI index | 3 m × 10 m | | MINDVI effective size is smaller than the highest spatial resolution |
| (Park et al., 2021) | WorldView-3 | ⸗ | ⸗ | Green (547.1 nm) NIR-1 (824.0 nm) | 1.24 m MS bands after pan sharpening 0.3 m × 0.3 m ((< 0.1 cm × 0.1 cm pixel) | NA | NA | proxy based band difference | NA | NA | NA |
| (Jamali and Mahdianpari, 2021) | Sentinel-2B | ⸗ | ⸗ | Band 2–8 | 10 m (Band 2, 3, 4, 8) 20 m for (Band5,6) | 45 m × 5 m; 21 m × 10 m PLP | NDVI and FDI | Supervised RF, SVM and GAN-RF) | 45 × 5 m | NA | RF 88 % SVM 84 % GAN-RF 96 % |
| (Kikaki et al., 2022) | PlanetScope, Sentinel-2 | ⸗ | ⸗ | All S2 bands expect band 9, 10 Planetscope; all bands | 10 and 20 m (S2) 3 m for PS | Citizen science, literature and social media | NDVI, NDWI, FAI, FDI, (SI), (NDMI), (BSI), NRD | Supervised Classification Developed $RF_{SS+SI+GLCM}$ model | 373 targets identified | NA | RFSS+SI + GLCM pixel accuracy 0.92 U-Net pixel accuracy 0.7 |
| (Hu, 2022) | Sentinel-2 | ⸗ | VIS-NIR | Band 2–8 in | Band 2–4, 8 (10 m) Band 5–7 (20 m) | Citizen science and literature | NA | Spectral Unmixing | NA | NA | NA |
| (Ciappa, 2022) | Sentinel-2 | ⸗ | VIS-NIR | Visible (bands 2, 3, 4), Red Edge (5, 6, 7) and NIR (8) | Band 2–4, 8 (10 m) Band 5–7 (20 m) | NA | NA | Spectral Difference | NA | NA | 59 % Vegetation, 16 % marine litter and 22 % mixed |
| (Simpson et al., 2022) | Sentinel-1 SAR | ⸗ | SAR C-Band 5.404 GHz | C-band | 5 m | Debris accumulated at Potpecko Lake Dam, Serbia | NA | Backscattering with different polarization | NA | NA | 75–85 % positive detection |
| (Olyaei et al., 2022) | Sentinel-2 | ⸗ | VIS-NIR, SWIR | Band 2,3,4,8,11 and 12 | Band 2,3,4 and 8 (10 m) Band 11 and 12 (20 m) | MARIDA datasets 3399 pixels of sentinel-2 for Plastic, 2797 pixels for seagrass | NA | SVF and RF | NA | NA | 88 % for SVF and 97 % for RF |
| (Taggio et al., 2022) | PRISMA | ⸗ | VIS-NIR-SWIR (175 out of 239 bands used) | VIS-NIR: 400–1010 nm (66 bands) SWIR: 920–2500 nm (173 bands) all bands used expect between 1350 and 1470 nm and 1800–1970 nm | 5 m (Pansharpened) | 5.1 m × 5.1 m (4 targets) 2.4 m × 2.4 m (4 targets) 0.6 m × 0.6 m (4 targets) | NA | Unsupervised K-Means and supervised LGBM | 5.1 m × 5.1 m | ~2.4 m × 2.4 m | LGBM 96 % and K-means 66 % |
| (Kremezi et al., 2022) | Sentinel-2 WorldView-2, WorldView-3 | ⸗ | VIS-NIR-SWIR | VIS-NIR (400–1040 nm) SWIR(1613 nm and 2202 nm) | Sentinel-2 fused with WorldView-2 (2 m) and | 10 m × 10 m (3 targets) 2.4 m × 2.4 m (4 targets) | NDVI, FDI, FAI, HI | Image Fusion and Image Interpretation | 10 m × 10 m | 0.6 m × 0.6 m | 99 % |

(*continued on next page*)

**Table 3** (*continued*)

| Reference | Sensor | Platform | Spectral range | Band used | Spatial resolution | In-Situ data | Indices used | Image classification | Largest detected plastic | Smallest detected target | Accuracy obtained |
|---|---|---|---|---|---|---|---|---|---|---|---|
| | | | | | WorldView-3 (4 m) | 0.6 m × 0.6 m (4 targets) | | | | | |
| (Nagy et al., 2022) | Sentinel-2 | ⸗ | ⸗ | All Bands 442 nm to 2202 nm | B2, B3, B4, B8 (10 m) and B5, B6, B7, B8a, B11, B12 (20 m) | 10 m × 10 m and 28 m in diameter target | NA | RF | 28 m diameter target | 10 m × 10 m | 99 % |
| (Sannigrahi et al., 2022) | Sentinel-2 A/B | ⸗ | ⸗ | B4, B6, B8, B11 | Band 4 and 8 (10 m) and Band 6 and 11 (20 m) | Greece<br>10 m × 10 m<br>5 m × 5 m<br>1 m × 5 m<br>2.4 m × 2.4 m<br>Cyprus<br>3 m × 10 m | FDI, PI, NDVI, kNDVI | SVM and RF | 23/33 plastic pixels detected Beirut<br>35/42 plastic pixels detected for Calabria | | 91 % RF |
| (Hui et al., 2023) | Sentinel-2 and WorldView-3 | ⸗ | ⸗ | All Bands 442 nm to 2202 nm | S2 10–20 m and WV3 1.24–3.7 m | Plastic bag per km2 area | FDI, NDVI, and SAM | Adjoint marginal sensitivity method | | | |
| (Duarte and Azevedo, 2023) | Sentinel-2 | ⸗ | ⸗ | All Bands 442 nm to 2202 nm | 10 m and 20 m | 209 Plastic containing pixels | FDI, NDWI, MNDWI, NDSI, WRI, MARI and OSI | Xgboost | | | 98 % |
| (Booth et al., 2023) | Sentinel-2 | ⸗ | ⸗ | Band 4, 6, 8, and 11 | Band 4,8 (10 m) and 6, 11(20 m) | MARIDA and PLP datasets | Marine Debris Map (MDM) | MAP-Mapper-HP<br>MAP-Mapper-Opt (U-Net) | | | MAP-Mapper-HP 95 %<br>MAP-Mapper-Opt 87 % |
| (Pichel et al., 2012) | Satellite<br>NOAA POES<br>MODIS<br>NOAA GOES<br>RADARSAT-1 SAR<br>TOPEX-Altimeter<br>King Air 90 aircraft -vissual, RGB, IR and LiDAR sensor | Spaceborne and Airborne | VIS, IR, SAR and LiDAR | | POES/GOES 1–4 km,<br>MODIS 250–1000 m,<br>Radarsat-125-100 m,<br>TOPEX 10–100 km and<br>LiDAR 1 cm | GhostNet buoy detected and tracked | NA | Manual identification and<br>tracking of eddies through altimeter, chlorophyll and SST satellite products | NA | NA | NA |
| (K Topouzelis et al., 2019) | SLANTRANGE 3p, Sentinel-1/2 A/B | ⸗ | VIS-NIR, SWIR and SAR | coastal (442–450 nm), blue (492–500 nm),<br>green (550–559 nm)<br>NIR (832–850 nm) | Slantrange 3P-4.84 cm<br>Sentinel-2 10 m<br>SAR 5 m | 10 m × 10 m (3 targets)<br>Plastic bottles, Plastic bags and Fish net | NA | Photointerpretation | 10 m × 10 m | 10 m × 10 m | NA |
| (Themistocleous et al., 2020) | VC HR1024 spectroradiometer, Phantom 4 Pro and Sentinel-2 | ⸗ | VIS-NIR-SWIR | Band S2 3,4,8,11,12 | S2 (Band 3,4 and 8) 10 m.<br>(Band 11 and 12) 20 m | Spectral Reflectance Evaluation<br>SVC HR1024 spectroradiometer. | (NDWI), (WRI), (NDVI), (AWEI), (MNDWI), (NDMI), (SR) | Developed PI and RNDVI | 50–110 m × 80 m fishing collar. | 3 m × 10 m | NDWI and SR identified 5 pixels<br>PI identified 7 pixels of targeted plastic |

(*continued on next page*)

**Table 3** (*continued*)

| Reference | Sensor | Platform | Spectral range | Band used | Spatial resolution | In-Situ data | Indices used | Image classification | Largest detected plastic | Smallest detected target | Accuracy obtained |
|---|---|---|---|---|---|---|---|---|---|---|---|
| (Gonzaga et al., 2021) | Sentinel-2, Drone images and Spectroscopy | ⸗ | ⸗ | Band S2 4,6,8,11,12 | (Band 4 and 8) 10 m. (Band 6, 11 and 12) 20 m | 9 Drone inspections | FDI, NDVI and PI | Supervised Naïve Bayes and Mixture Tuned Matched Filtering (MTMF) | NA | NA | Highest user accuracy 57.14 %. |
| (Papageorgiou et al., 2022) | Sentinel-2, DJI Phantom 4 RTK drone, Bayspec Hyperspectral Imager | ⸗ | ⸗ | S2 Bands 4,6,8,11,12 and Hyperspectral Imager (400–1000 nm) | Band 4 and 8 (10 m) and Band 6, 11 and 12 (20 m) Hyperspectral Imager 3 cm | 10 m × 10 m 5.1 m × 5.1 m 2.4 m × 2.4 m 0.6 m × 0.6 m 28 m in diameter | FDI, NDVI | Spectral unmixing | Target with 28 m in diameter | 10 m × 10 m | |
| (Hu et al., 2023) | Spectroscopy, Aerial Photograph, MODIS, MERIS, and Landsat | ⸗ | VIS-NIR 400–900 nm | Blue, Green, Red and NIR | Aerial 0.5 m, MODIS Aqua/ Terra-250 m, MERIS 300 m And Landsat 30 m | Citizen Science | NA | Spectral Unmixing of Pixels | 21.7 $km^2$ aggregated debris | NA | NA |
| (Tasseron et al., 2021) | Spectroscopy, Sentinel-2 and Worldview 3 | Spaceborne and Lab based | VIS-NIR- SWIR | Spectroscopy (400 to 1700 nm) Senitnel-2 Band 5, 8 10 Worldview 3 band 4,5,6, 10, 12 nm | VIS-NIR pixel size 20 × 10 um, NIR-SWIR pixel size 18.7 × 18.7 um S2 band 8 (10 m), band 5 &10 (20 m) worldview MS 1.2 m and SWIR 3.7 m | Spectral signature Evaluation | NDVI and FDI | Linear Discriminant Analysis | NA | NA | NA |
| (Moshtaghi et al., 2021) | Sentinel-2 and spectral cameras | ⸗ | VIS-SWIR | 350–2500 nm | NA | Spectral signature of different types of wet and dry plastic | FDI and NDVI | Spectral Evaluation for band selection | 1070 nm is the best to discriminate plastics <5 cm | NA | NA |
| (Goddijn-Murphy and Dufaur, 2018) | VIS-SWIR spectrum spectral cameras | Lab Based | VIS-SWIR | 700 to 1400 nm for NIR 1400 3000 nm for SWIR | NA | spectral signature evaluation | NA | Optical Reflectance model development | NA | NA | NA |
| (Serafino and Bianco, 2021) | X-band Radar | Mounted on Building | X-band | 3.75–2.4 cm Wavelength 7.0–11.2 GHz Frequency | NA | Small Garbage Island | NA | Signal Processing | 13 × 4 cm in diameter | 1 × 1 m | NA |

further aid in detecting FMML.

### 3.3. Spectral resolution

High spectral resolution sensors are required to obtain accurate absorption or reflection of different materials (Chavez, 1988; Pichel et al., 2012). Similarly, for the detection of FMML, understanding its spectral signature across different wavelengths of the electromagnetic spectrum is also crucial (Hu, 2022; Mace, 2012). For remote sensing data, most of the progress has been made in VIS, NIR and SWIR spectral sensors (Kikaki et al., 2020; Nikolai Maximenko et al., 2019; Mukonza and Chiang, 2022; Veettil et al., 2022). Spectral reflectance measurements over these wavelengths have been made through in-situ or lab-based experiments, UAVs, manned aircraft, and satellite multispectral sensors (Table 3). The accurate spectral reflectance of plastic enables us to identify the FMML in the marine environment. The macro plastic and other floating materials reflect light in NIR and SWIR bands, while water absorbs most in these wavelengths. Due to these spectral properties, FMML is visible from space (Biermann et al., 2020; Garaba et al., 2018; Goddijn-Murphy and Dufaur, 2018; Hu, 2022).

We observed that some of the studies used the lab-based spectroradiometer in visible, NIR, and SWIR spectra to study the spectral reflectance properties of different plastic materials (Goddijn-Murphy and Dufaur, 2018; Moshtaghi et al., 2021; Tasseron et al., 2021). Similarly, sensors with VIS, NIR, and SWIR wavelengths have also been mounted on airborne platforms to identify FMML in the ocean (Balsi et al., 2021; Garaba and Dierssen, 2018; Hueni and Bertschi, 2020; Tasseron et al., 2021). Additionally, most studies used spaceborne multispectral remote sensing data with different spectral bands in VIS, NIR, and SWIR spectra, which can be used to identify the FMML. The spectral evaluation of plastic in the lab helps to select the best-performing bands of multispectral satellite data in the identification of FMML (Biermann et al., 2020; Tasseron et al., 2021), and FMML rafts composition is further confirmed from very high-resolution spectral data by drone surveys (Almeida et al., 2023; Freitas et al., 2022; Garaba et al., 2018). For example, Hu (2022) assessed the spectral characteristics of Sentinel-2 bands in VIS and NIR spectra to examine the spectral shape and effect of mixed pixels for FMML identification and detection. The Sentinel-2 data is used in FMML identification due to their unique multispectral bands, but bands in NIR and SWIR regions (Band 4, 8, 11, 12) are widely used due to their unique characteristics of discriminating the FMML objects from other floating objects (Table 3).

### 3.4. Plastic detection method

According to different studies, different methods have been employed to detect the FMML using remote sensing data. The detection algorithms here used spectral signatures of marine plastic for carefully selecting the spectral bands in VIS, NIR, and SWIR spectra to create feature extraction indices and to develop image classification algorithms.

#### 3.4.1. Indices used

Band rationing is a straightforward and powerful technique in multispectral remote-sensing image processing (Hu, 2022). Other than the applications of discrete spectral bands, different spectral indices highlighted their efficacy in identifying FMML. These indices were developed using VIS, NIR, and SWIR spectrums (Table B1). Biermann et al. (2020) developed Floating Debris Index (FDI) (Eq. 12) using Sentinel-2 band 4 (Red), band 6 (Rededge2), band 8 (NIR), and band 11 (SWIR 1). Biermann et al. (2020) also used the Normalized Difference Vegetation Index (NDVI) (Tucker, 1979) (Eq. 3) based on Sentinel-2 band 4 and band 8 to identify and classify the vegetation cover. FDI revealed the discrepancy in spectral signatures of floating objects and ocean water, and NDVI can detect the difference between plastics, vegetation, driftwood, and seafoam. When FDI and NDVI are used together, FMML can be detected at the sub-pixel level (Biermann et al., 2020). Themistocleous et al. (2020) developed the Plastic Index (PI) (Eq. (11)) and Reversed Normalized Difference Vegetation Index (RNDVI) (Eq. (7)) using band 4 and band 8 of Sentinel-2 satellite images. PI and RNDVI can differentiate the plastic target from water, but PI shows better results as plastic targets give higher values from 0 to 1 during FMML detection. Similarly, Kremezi et al. (2021) evaluated the spectral values of FDI, NDVI, and hydrocarbon index (HI), and developed their own index using VIS and NIR bands with central wavelengths (at 492, 596, 719,781, and 951 nm) for hyperspectral PRISMA pan-sharpened data (Table B1). The HI index (Eq. (13)) can also identify plastic from other floating objects (Kremezi et al., 2022). Another index, Modified Infrared Normalized Vegetation Index (MINDVI) (Eq. (10)), was proposed by Khetkeeree and Liangrocapart (2021) using Sentinel-2 (band 8, 11, 12) data and claimed that it can identify plastic targets smaller than image resolution. The Floating Algae Index (FAI) developed by Hu (2009) (Eq. (14)) can detect and differentiate floating vegetation from other debris, given sufficient pixel coverage. Similarly, Sannigrahi et al. (2022) utilized the Kernel Normalized Difference Vegetation Index (kNDVI) (Eq. (15)), by B4 and B8, which is effective in detecting floating plastic in open ocean. An interesting Marine Debris Map (MDM) index proposed by Booth et al. (2023) gives the average probability of a pixel containing floating marine litter.

Most of the studies considered the spectral signature of plastic by using background knowledge of FDI, NDVI, PI, etc., to develop their image classification models for the detection and identification of FMML (Basu et al., 2021; Duarte and Azevedo, 2023; Gong et al., 2022; Jamali and Mahdianpari, 2021; Mifdal et al., 2021; Moshtaghi et al., 2021; Sannigrahi et al., 2022; Tasseron et al., 2021). Spectral indices values depend on different floating plastic materials that co-exist with other non-plastic materials. Furthermore, indices such as Normalized Difference Plastic Index (NDPI) (Guo and Li, 2020), Advanced Plastic Greenhouse Index (APGI) (Zhang et al., 2022), Advanced Hydrocarbon index (HI) (Garaba and Dierssen, 2018) and relative-absorption band depth (RBD) index (Asadzadeh and de Souza Filho, 2016) could also show their potential in detection of FMML. Thus, different indices operate in their respective circumstances; however, the performance appears exceptionally dependent on the spatial and spectral resolution of remote sensing data, the size of aggregated plastic targets, and the concentration of suspended particles.

#### 3.4.2. Image classification method

Different image classification algorithms have been used to detect floating marine litter in the ocean. For detection, identification, and quantification, different authors tested image interpretation, band rationing, and supervised and unsupervised image classification algorithms (Table 3). In supervised classification, pixels containing plastic litter (training samples) are manually selected, and the rest of the images were classified on that basis. Few studies have used RGB images to identify plastic, and FDI and NDVI to obtain the shape and spectral signature of plastic using multi-spectral remote sensing data. Later, they developed deep-learning models using spectral signatures (de Vries et al., 2021; Garcia-Garin et al., 2021; Wolf et al., 2020). In other cases, the authors have also employed CNN deep learning models (Almeida et al., 2023; Garcia-Garin et al., 2021), naïve Bayes (Biermann et al., 2020), Mixture Tuned Matched Filtering (MTMF) (Gonzaga et al., 2021), random forest (RF) (Jamali and Mahdianpari, 2021; Kikaki et al., 2022; Olyaei et al., 2022), Support vector machine (SVM) (Basu et al., 2021; Mifdal et al., 2021; Sannigrahi et al., 2022), generative adversarial network-random forest (GAN-RF) (Jamali and Mahdianpari, 2021), U-Net (Mifdal et al., 2021), Semi-Supervised Fuzzy c-means (SFCM) (Basu et al., 2021) and Light Gradient Boosting Model (LGBM) (Taggio et al., 2022) and Extreme Gradient Boosting (Xgboost) supervised learning algorithms (Duarte and Azevedo, 2023) and unsupervised K means and Fuzzy c-means Clustering Algorithm (Basu et al., 2021). Another study by Wolf et al. (2020) used two separate CNN models (PLD-CNN and PLQ-

CNN) to identify and quantify FMML using very high-resolution remote sensing data. For some study areas, the researcher manually assessed the possibility of FMML by RGB interpretation along with the spectral indices (FDI and NDVI) to develop and train their models (Biermann et al., 2020; Gonzaga et al., 2021; Kikaki et al., 2022; Mifdal et al., 2021). Biermann et al. (2020) discriminated the FMML from other floating materials by leveraging the spectral shape and later used the Naïve Bayes classification algorithm to classify it from other floating materials. Similarly, Tasseron et al. (2021) evaluated the spectral values of plastic, discriminated them from other floating objects in water using Linear Discriminant Analysis (LDA), and later compared the results with multispectral bands of Sentinel-2 and Worldview 3 satellites data. In another study, de Vries et al. (2021) employed Faster R-CNN (FRCN) and YOLOv5 image detection model on the video footage to detect and quantify the FMML. Similarly, Taggio et al. (2022) used unsupervised the K-Means and supervised LGBM models on pansharpened PRISMA data to detect and quantify the FMML. Duarte and Azevedo (2023) trained Xgboost model on the pixel containing plastic litter along with spectral bands and indices to detect and quantify the FMML. Booth et al. (2023) used U-Net based MAP-Mapper image classification method to assess the concentration of potential marine debris in multiple location. Armitage et al. (2022) employed YOLOv5 object detecton model on the video footage tp detect and quantify the FMML. These FMML models were trained on a balanced dataset from the training samples to classify and differentiate the FMML from water, wood, and other floating objects. Moreover, from the bibliographic review, we found that 9 studies used image interpretation, 19 used supervised learning models, 5 developed new indices and 9 evaluated the spectral signatures for the identification and discrimination of FMML from other floating materials (Table 3).

### 3.5. Accuracy assessment

Generally speaking, FMML identification accuracy depends on spatial resolution, spectral bands, aggregated plastic target size, oceanic condition, and the method used (Nikolai Maximenko et al., 2019; Veettil et al., 2022; Wolf et al., 2020). It is also influenced by the discrimination of the FMML from water, ships, wood, and other floating objects. Different studies claimed their accuracy on different sets of grounds. Some studies focused on identifying FMML, and some tried to discriminate it from other floating objects in the ocean. Biermann et al. (2020) claimed an accuracy of about 83 % by employing FDI and NDVI together to identify the FMML, and later used spectral values and Naïve Bayes classier to discriminate plastic from seaweed and sea foam by using the multispectral Sentinel-2 data. A similar study by Jamali and Mahdianpari (2021) obtained an accuracy of about 88 %, 84 %, and 96 % for random forest (RF), support vector machine (SVM), and a deep learning model Generative Adversarial Network-Random Forest (GAN-RF) respectively. Mifdal et al. (2021) have also used SVM, RF, CNN U-Net, and Naïve Bayes Classifiers on a balanced dataset and claimed that CNN U-Net was best performed with an accuracy of 84.28 % but for Kikaki et al. (2022) the accuracy of CNN U-Net 70 % is comparatively lower than their own developed RFSS+SI + GLCM with accuracy 92 % using the same kind of data and parameters. Similarly, Sannigrahi et al. (2022) employed SVM and RF for image classification by using different indices and spectral bands as predictors, and found RF performed best with an accuracy of 91 % for detecting FMML. Another study by de Vries et al. (2021) used YOLOv5 to accurately identify 111 of 416 plastic targets larger than 50 cm but could not identify targets smaller than 5 cm from video footage, while Armitage et al. (2022) obtained an accuracy of 95.2 % for plastic litter >1 cm. Booth et al. (2023) claimed an accuracy of 95 % by using the U-Net-based MAP-Mapper image classification method to assess the concentration of potential marine debris in multiple locations. Taggio et al. (2022) obtained an accuracy of about 96 % for LGBM model to detect the FMML greater than ~0.6 m × 0.6 m. Duarte and Azevedo (2023) used the Xgboost model on Sentinel-2 data to detect and classify the FMML and differentiate it from other floating materials with an accuracy of 98 %. The image interpretation method also claimed accuracy in the detection of FMML. Garcia-Garin et al. (2020b) conducted aerial (6300 images) and vessel-based surveys and claimed 99 % of the detected FMML items were made of plastic. In another study, Garaba and Dierssen (2018) identified 118 FMML objects out of 150 by overlapping SWIR-SASI images on RGB images over the GPGP region. Other than these image classification methods, Serafino and Bianco (2021) explained the accuracy of X-band radar which depends on the ocean state, target size, and signal strength which is also applicable to the use of LiDAR (Feygels et al., 2017). Similarly, Goddijn-Murphy and Williamson (2019) explored the potential use of utilizing TIR sensor data, demonstrating its effectiveness in distinguishing FMML. Another study by Simpson et al. (2022) used Sentinel-1 SAR data to monitor accumulated plastic island with an accuracy of 75–85 %. From the bibliographic review, we observed that the supervised learning models using background knowledge of different indices for detection of FMML obtained an accuracy between 60 % and 93 % (Table 3).

## 4. Discussion

In this systematic review, we have conducted descriptive literature analysis using all available studies that used remote sensing data to detect floating macro marine litter (FMML) in the ocean water. The literature was searched on Web of Science (WoS) and Scopus databases using the selected keywords (Fig. 1). Initially, we obtained 874 studies, and after removing 223 duplicates, 650 studies were left for initial screening (titles and abstracts) (Fig. 2). After completing the initial screening, we retrieved 182 studies for full-text screening. Finally, we retained 44 papers out of 48 for describing the results (or data sets) during the data extraction that met our inclusion criteria in the systematic review. Two authors did the initial and final screening and extracted the data from all the eligible studies independently (Sections 2.2 and 2.3). The extracted data allows us to identify and explain various combinations of sensors, platforms, spatial resolution, spectral resolution, in-situ data, indices used, detected FMML targets, the method used to identify FMML, and the accuracy obtained.

### 4.1. Recent FMML detection remote sensing studies

The detection of FMML using remote sensing data has been the subject of great attention due to its serious concerns associated with the marine environment and human health. From the studies reviewed, we observed that several different methodological approaches have been used to detect and identify FMML. These methods used different remote sensing data sets, including in-situ plastic targets and spectral reflectance data to develop plastic detection methods. Lab-based experiment design studies were conducted to extract the meaningful spectral measurement of different plastic materials in the marine environment for different sensors (Goddijn-Murphy and Dufaur, 2018; Moshtaghi et al., 2021). Another experimental design study deployed artificial plastic targets (made of plastic bottles, bags, and fish nets) in the coastal waters. Then, they identified them by photointerpretation method to explore the effectiveness of VIS, NIR, and SWIR spectral ranges of the hyperspectral airborne imager (SLANTRANGE 3p) and multispectral satellite data (Sentinel-1&2 A/B) (K Topouzelis et al., 2019; Topouzelis et al., 2020b). Furthermore, a few studies used different high-resolution sensors mounted on airborne and vessel-based platforms to identify plastic floating on the sea surface by images visually (Garaba et al., 2018; Garcia-Garin et al., 2020b; Kikaki et al., 2020; Lebreton et al., 2018; Pichel et al., 2012; Simpson et al., 2022). The photo and visual interpretation methods are time-consuming, have low synoptic coverage, are expensive, and require a trained observer. These experimental studies validated the concept of identification and classification of marine plastics using multispectral remote sensing data aided by in-situ and high-resolution aerial images.

The most recent development has been made in spectral remote sensing employing VIS, NIR, and SWIR wavelengths for identifying and detecting floating plastic on the ocean surface. However, the thermal Infrared (TIR) spectrum can also be used to identify the floating materials on the ocean surface as they emit and reflect different temperature values from their surroundings. Goddijn-Murphy and Williamson (2019) used the emissivity values of plastic and water to identify floating plastic in the ocean using TIR data. However, this approach can only give the best results when the difference in air-sea temperature is significant. Similarly, the use of LiDAR can be used for quantification of the aggregated large plastic targets at the water surface, sink to the bottom, or in the water column as the backscatter values of laser light from different objects with different spectral values are detected (Feygels et al., 2017; Lebreton et al., 2018). The 3D visualization using LiDAR data provides a volume estimate and size distribution of the aggregated marine plastic. The SAR remote sensing data can also detect larger aggregated plastic targets by examining the intensity of the backscattered signal from the plastic and the surrounding water (Savastano et al., 2021; Simpson et al., 2022; K Topouzelis et al., 2019). For example, Simpson et al. (2022) used Sentinel-1 SAR data to monitor accumulated plastic islands floating on the water surface. Moreover, X-band radar can also identify, discriminate, and follow the trajectory of aggregated FMML on the ocean surface (Serafino and Bianco, 2021). However, the ability of X-band radar depends on the reflective intensity of the floating materials and decreases as the targets move away and signal strength weakens at the antenna. It also observed that TIR, X-band radar (mounted or airborne), and LiDAR could only perform well when the atmospheric and oceanic conditions are normal. The opposite is in the case of SAR data due to changes in backscatter intensities in different sea surface roughness.

Another methodological advancement has been made in the development of different indices to detect floating materials on the ocean water surface. The spectral indices can robustly identify and separate the floating aggregated materials and ocean water. These indices used the background knowledge of spectral signatures of plastic materials in the VIS, NIR, and SWIR range of the electromagnetic spectrum to identify the shape and size of the floating patch (Tables 3 & B1). For example, Biermann et al. (2020) suggested the Floating Debris Index (FDI) that can identify the pixels dominated by floating materials at a sub-pixel scale and further classify the aggregation made up of natural materials or plastic by using NDVI and image classification method. The Plastic Index (PI) and Reversed Normalized Difference Vegetation Index (RNDVI), developed by Themistocleous et al. (2020), can detect all kinds of smaller floating plastic. Similarly, Khetkeeree and Liangrocapart (2021) developed the Modified Infrared Normalized Vegetation Index (MINDVI), which can effectively detect FMML smaller than the image resolution. Kremezi et al. (2021) used pan-sharpened PRISMA (5 m) hyperspectral satellite data, and developed an index in VIS and NIR bands (492, 596, 719,781, and 951 nm) that can discriminate between the floating plastic and non-plastic floating targets (Table 3). The hydrocarbon index developed by (Kühn et al., 2004) can distinguish floating vegetation and other plastic (Garaba et al., 2018; Kremezi et al., 2022). The Floating Algae Index (FAI) developed by Hu (2009) can detect the floating vegetation from other debris, given sufficient pixel coverage (Kikaki et al., 2022; Kremezi et al., 2022). Similarly, Booth et al. (2023) developed the Marine Debris Map (MDM), which provides the average probability of the pixel containing marine debris. The accuracy of these indices depends on the bands' spectral range and the spatial resolution of different sensors. These band ratio techniques are well used to identify the marine debris containing pixels in the remote sensing data, but these spectral indices cannot stand alone to discriminate between different plastic materials from other floating materials. The performance of these spectral indices can be improved by using hyperspectral remote sensing data with high spatial resolution, acquired during suitable conditions on the sensor and ground.

Another advancement has been made in training different supervised and unsupervised image classification methods for identifying, detecting, and quantifying FMML in the ocean. For training and testing on remote sensing data, most studies have used in-situ plastic targets, spectral values of plastic, and various spectral indices as predictors of different image classification methods for FMML. From the literature, most of the machine learning methods trained on Sentinel-2 data (Biermann et al., 2020; Booth et al., 2023; Ciappa, 2022; Duarte and Azevedo, 2023; Gonzaga et al., 2021; Jamali and Mahdianpari, 2021; Kikaki et al., 2022; Mifdal et al., 2021; Nagy et al., 2022; Olyaei et al., 2022) but a few have used UAV-drone (Balsi et al., 2021; Garcia-Garin et al., 2021; Mace, 2012; Wolf et al., 2020) and vessel-based high-resolution images (Armitage et al., 2022; de Vries et al., 2021). These methods include Support vector machine (SVM), support vector regression (SVR), Random Forest (RF), semi-supervised fuzzy c-means (SFCM), Naïve Bayes, Convolutional Neural Network (CNN) U-Net, Mixture Tuned Matched Filtering (MTMF), Generative Adversarial Network-Random Forest (GAN-RF), Tensor Flow Object Detection (FRCNN and YOLOv5), Plastic Litter Detector and Quantifier (APLASTIC-Q), Extreme Gradient Boosting (Xgboost), Light Gradient Boosting Model (LGBM) and MAP-Mapper (U-Net) (Table 3). Despite the data limitation and uncertainty, these advanced machine learning and clustering methods could demonstrate their application and usability in the detection of floating marine litter. These supervised machine learning algorithms can enhance their accuracy in the detection of floating plastic in the ocean using in-situ targets, spectral signature, indices, and high resolution (spectral and spatial) remote sensing data in stable atmospheric and oceanic conditions. The image classification performance of these models can also be increased by increasing the number of images with plastic targets for training and testing the models.

### 4.2. Gaps and limitations

Even though satellite data has shown its potential for studying coastal and marine ecosystems with a great synoptic view and fine spectral temporal resolution, they still have some limitations. Some satellite data have a coarser spatial resolution for detecting aggregated FMML targets at the sub-pixel level. Some remote sensing satellites have significant measurement uncertainty due to noise in spectral bands. Remote sensing data acquisition during normal atmospheric and oceanic conditions is vital, including VIS, NIR, SWIR, TIR, and LiDAR. The preprocessing, such as atmospheric correction, sun glint, and the clouds masking on the satellite data, can significantly affect the accuracy of marine plastic detection. These constraints of using satellite data should be considered when implementing marine plastic detection methods such as indices, spectral classification methods, unsupervised clustering, and more complex supervised classification algorithms like artificial intelligence and machine learning.

The expanded use of UAV drones over airborne manned vehicles (aircraft) in terrestrial research also underlines its importance in litter detection on beaches and in the ocean. The aerial surveys from high-wing platforms are more expensive to carry out despite the fact they can offer a vast coverage and valuable abundance estimations for macro plastic marine litter. On the other hand, UAV drones have greater flexibility in carrying a wide range of sensors developed for specific target-related assessments of environmental concerns. The UAV-Drones can provide high-resolution (spatial and spectral) data due to their low flight height to identify macro marine plastic litter, but they have a limited weight capacity. The drone also has a limited battery, reducing its useability to carry out remote sensing data acquisition over a larger area.

The absence of adequate and high-quality in-situ data for the training and developing of plastic detection methods is possibly the most significant challenge. In real-world scenarios, the aggregated plastic patches floating on the ocean surface are very sparse, which poses significant impediments to remote sensing data availability over the area and depends on the oceanic condition during the data acquisition process. For this, OceanScan (OceanScan.org) provides a global database of

carefully selected in-situ and matching satellite images at the same time and space. The acquired satellite data with the slightest cloud cover and having a wave-tide height of >3 m in the ocean can significantly reduce the useability of the acquired data. As a result, the significant number of in-situ plastic data and high-quality spectral measurements of floating marine litter are critical for developing effective remote sensing methodologies for marine litter detection.

### 4.3. Further work

So far, the researcher's primary focus has been dedicated to the identification of marine plastic litter on water surfaces and beaches using remote sensing data, although attempts to detect and characterize the marine litter problem in all interconnected regions are underway. The first initiative should be developing a new infrastructure to prevent plastic litter from entering into oceans and implementing relevant policies for marine littering. In addition, it is also necessary to quantify the sources of marine plastic pollution, their trajectory, and the present amount in the world's oceans. For identification, most of the methods developed have certain levels of uncertainty and are at a low level of maturity due to data limitations. Future developments will include inexpensive, sophisticated data acquisition technology for improving remote and autonomous monitoring and expanding monitoring to all regions. The development of novel and integrated solutions to monitor the changes and distribution of marine debris globally using remote sensing data and in-situ data is also urgently required.

In addition, the space agencies (ESA, NASA, NOAA, JAXA, etc.) and the different scientific communities are working on the development of an integrated platform with different airborne sensors in the VIS, NIR, and SWIR ranges, including SAR, TIR, and LiDAR to provide high-resolution remote sensing data ahead of spaceborne sensor's abilities. An ideal remote sensing data (VIS, NIR, and SWIR) must have less than or equal to 1-m spatial resolution and have different spectral bands to accurately monitor and quantify the marine plastic entering the ocean in the future. Improvements in sensor quality will also enable the discrimination between floating marine debris and lookalikes. The improved sensors will also have high SNR values since floating material's spectral responses are similar to the noise in low SNR bands and sensors. A coordinated network of high-resolution sensors mounted on UAV drones could also help scan larger areas to detect marine plastic pollution floating in the ocean. The long battery life, network autonomy, weight capacity, and cost-effective platforms and sensors can enhance the capability of advanced monitoring of FMML using UAV drones. Future high-resolution hyperspectral remote sensing satellite missions in VIS, NIR, and SWIR spectra include HyspIRI (30–60 m), EnMap (30 m), GHOST (30 m), CHIME (30 m), SHALOM (2.5–10 m) and multispectral Pléiades satellite mission (2 m). These new missions and existing ones can significantly enhance our capacity to monitor the floating marine litter in the ocean (Livens et al., 2022). Furthermore, future research utilizing multispectral or hyperspectral remote sensing data for the detection of FMML can employ indices such as the Normalized Difference Plastic Index (NDPI) (Guo and Li, 2020), Advanced Plastic Greenhouse Index (APGI) (Zhang et al., 2022), Advanced Hydrocarbon index (HI) (Garaba and Dierssen, 2018) and relative-absorption band depth (RBD) index (Asadzadeh and de Souza Filho, 2016).

The growing number of studies dedicated to remote detection of floating marine plastic pollution through remote sensing data highlighted the significance of this research topic. Like in the past, there are several ongoing and upcoming projects in collaboration between the world's research community for advancing the use of remote sensing data for this global issue. For example, advancement has been made by the Plastic Litter Project 2018, 2019, 2020, 2021, 2022 (Papageorgiou et al., 2022; PLP, 2023; K Topouzelis et al., 2019; Topouzelis et al., 2020a) and MARIDA (Kikaki et al., 2022) for helping other researchers explore the underlying opportunities in the detection and quantification of plastic litter in the ocean. Similarly, the European Space Agency (ESA) has launched multiple projects under the Discovery Campaign on Remote Sensing of Plastic Marine Litter. These projects include Remote Sensing of Plastic Marine Litter, Artificial Intelligence and drones supporting the detection and mapping of floating aquatic plastic litter (AIDMAP), Plastic Litter Project (PLP), FRONTAL, SPOTS, HyperDrone, and TRACE. All these initiatives fall under ESA's Open Space Innovation Platform (OSIP) funding campaign (ESA, 2021), which sponsors innovative ideas for marine plastic detection using remote sensing. Similarly, the Ocean Clean-up project carried out different research projects, such as Remote Sensing of Marine Litter (RESMALI project) in collaboration with ESA for developing and scaling remote sensing-based technologies for monitoring plastic pollution in the ocean (de Vries et al., 2021; The Ocean Cleanup, 2023). Furthermore, other organizations, like NASA, also launched Research Opportunities in Space and Earth Science (ROSES) programs, including remote detection of marine litter (NASA, 2022). Other research organizations such as Portugal Space Agency and Italian National Research Council (CNR) have also funded some projects focused on this remote sensing of floating marine litter. The task force on remote sensing of marine debris by the International Ocean Colour Coordinating Group (ICCOG) supports international collaboration to standardize different methods used to detect FMML (ioccg.org).

## 5. Conclusion

The global issue of persistent plastic litter, originating from different sources and transported by rivers to oceans, has posed serious biological, ecological, and chemical effects on marine ecosystems. The present systematic review aims to discuss the identification of floating macro marine litter (FMML) in the ocean using remote sensing data. This paper has described the usability of different sensors with different spatial, temporal, and spectral characteristics for detecting marine plastic litter, as well as their strengths and limitations.

For future study, the development of an integrated method to achieve precise, effective, robust, and large-scale monitoring of FMML by employing a suite of suitable remote sensing sensors (active & passive) and appropriate ground survey conditions should be conducted. The sensors should have a high spatial resolution (<1 m) to detect the smallest possible FMML patch and have different spectral bands, which can optimize discrimination between the different FMML types (plastic, wood, seaweed, etc.) in different oceanic conditions. The sensors should also utilize the unique spectral characteristics of VIS, NIR, and SWIR wavelength ranges to employ different indices and image classification methods. A complete technique to detect macroplastic includes VIS spectrum for object detection, NIR (i.e., 1070 nm) for separating them from water, and SWIR (i.e., 1192–1215, 1660–1730 nm) for classifying different floating objects and macroplastic. The active TIR, SAR, LiDAR, or X-band Radar sensor data shows their potential for detecting floating marine plastic depending on the strength of the signal received or the backscatter values depending on the sensor used. The SAR or TIR data can supplement the optical data for plastic detection, while Radar or LiDAR data can be used to follow the trajectory and volume quantification of plastic in different columns of the ocean, respectively. The development of future multi-spectral sensors for FMML detection should utilize the unique spectral values of different plastic materials in the ocean. Additionally, the time and space for image acquisition and in-situ data sampling should be carried out during clear skies and stable ocean conditions. The in-situ plastic target samples should be significant in number to train the image classification method to further enhance FMML detection accuracy. Moreover, an up-to-date multi-class image classification algorithm should be developed and employed to accurately classify the macro plastic from other floating materials. In conclusion, high-resolution remote sensing data from a viable sensor combination (multi- or hyperspectral imager), sufficient in-situ data, and validated spectral signature are required to monitor FMML with a real-time/near real-time automatic detection algorithm. Although these technologies are useful, more research using airborne TIR, SAR, or

LiDAR sensors in combination with optical sensors will likely overcome the physical and technological barriers of optical remote sensing data for detection and quantification of marine litter. Due to the novelty of the research area, more extensive research is needed to be conducted during different sea states for floating or submerged marine plastic using different airborne sensors to validate satellite data.

## CRediT authorship contribution statement

**Muhammad Waqas:** Conceptualization, Data curation, Methodology, Formal analysis, Writing – original draft. **Man Sing Wong:** Supervision, Conceptualization, Resources, Writing – review & editing. **Alessandro Stocchino:** Writing – review & editing. **Sawaid Abbas:** Methodology, Writing – review & editing. **Sidrah Hafeez:** Methodology, Data curation. **Rui Zhu:** Writing – review & editing.

## Declaration of competing interest

The authors declare that they have no known competing financial interests or personal relationships that could have appeared to influence the work reported in this paper.

## Data availability

Data will be made available on request.

## Acknowledgements

This research was supported in part by the General Research Fund (project ID 15609421 and 15603920), and the Hong Kong Ph.D. Fellowship Scheme from the Research Grants Council of Hong Kong; and Environment and Conservation Fund (project ID: 2021-107; A multi-source remote sensing based technique for monitoring oil spills). M. S. Wong thanks the support from the Research Institute for Land and Space (project ID 1-CD81), the Hong Kong Polytechnic University. A. Stocchino thanks the support from the General Research Fund (project ID 15216422) from the Research Grants Council of Hong Kong.

## Appendix A

**Table A1**
List of general inclusion criteria considered to assess the risk of biasness and quality assessment of the eligible studies.

| Key criteria | General inclusion criteria | Risk of biasness | Quality assessment |
|---|---|---|---|
| Data used | Can we be confident in the characterization of data used?<br>List of major considerations:<br>1. Remote sensing data acquisition described<br>2. Characteristic of the sensor used<br>3. Spatial resolution must be ≤10 m<br>4. In-situ data used to supplement the remote sensing data considered<br>5. Oceanic conditions during the data acquisition considered<br>6. Spectral signature profile of the plastic materials is considered | -LOW risk: all factors were considered.<br>-PROBABLY LOW: All factors were considered but oceanic conditions is not considered during data acquisition and spectral profiling of plastic materials.<br>-PROBABLY HIGH: In-situ data not used along with spectral values of plastic and oceanic condition.<br>-HIGH risk: All general criteria were not considered or partially considered | -Very High Quality: All general criteria factors considered<br>-High Quality: general criteria (5) or (6) not considered<br>-Moderate Quality: general criteria (3) or (4) not considered along with (4) or (5)<br>-Low Quality: general criteria (3), (4) and (6) not considered and others partially considered |
| Method used | Can we be confident on the detection method used?<br>List of major considerations:<br>1. Detection or monitoring methods for floating plastic described clearly (Image Classification/image interpretation/index-based/ artificial intelligence<br>2. In-situ data considered in detection methods<br>3. Methodological development and assessed different methods<br>4. Detected plastic target size reported and assessed visually | -LOW risk: methodological development was reported, and the outcome assessed visually based on ground truth data and the size of the detectable object was reported.<br>-PROBABLY LOW: Outcome assessed based on ground truth data and visual analysis; however, the size of the detectable object was not reported.<br>-PROBABLY HIGH risk: Outcome was not assessed based on ground truth data/visual analysis<br>-HIGH risk: Outcomes did not detect the plastic target | -Very High Quality: All general criteria factors considered<br>-High Quality: general criteria (3) or (4) not considered<br>-Moderate Quality: general criteria (2) not considered<br>-Low Quality: general criteria (2), (3) and (4) not considered and others partially considered |
| Accuracy obtained | Were all measured outcomes reported?<br>List of major considerations:<br>1. Pre-defined outcomes of the study discussed<br>2. Deployed plastic target size detected by the method used<br>3. Accuracy of the method used discussed<br>4. Limitation of the method used discussed<br>5. Uncertainty of the data used discussed | -LOW risk: All the studies' pre-defined outcomes and findings are reported.<br>-PROBABLY LOW: Insufficient information about the uncertainty of the data used discussed to judge the outcomes<br>-PROBABLY HIGH risk: The size of deployed targets detected less than their actual size<br>-HIGH risk: Not all pre-defined outcomes and findings were reported, and no accuracy and limitation of the data and method used discussed. | -Very High Quality: All factors considered<br>-High Quality: general criteria (4) or (5) not considered<br>-Moderate Quality: general criteria (2) and (3) along with (4) or (5) not considered<br>-Low Quality: general criteria (2), (3) and (4) not considered and other partially considered |

**Table B1**
List of all the indices used in different studies.

| Indices | Reference | Eq. no |
|---|---|---|
| $NDWI = \frac{Green - NIR}{Green + NIR}$ | (Duarte and Azevedo, 2023; Khetkeeree and Liangrocapart, 2021; Kikaki et al., 2022; Themistocleous et al., 2020) | Eq. (1) |
| $WRI = \frac{Green + RED}{NIR + SWIR2}$ | (Themistocleous et al., 2020) | Eq. (2) |

(*continued on next page*)

**Table B1** (*continued*)

| Indices | Reference | Eq. no |
|---|---|---|
| $NDVI = \frac{NIR - RED}{NIR + RED}$ | (Basu et al., 2021; Biermann et al., 2020; Gonzaga et al., 2021; Hui et al., 2023; Jamali and Mahdianpari, 2021; Kikaki et al., 2022; Kremezi et al., 2022, 2021; Mifdal et al., 2021; Moshtaghi et al., 2021; Papageorgiou et al., 2022; Sannigrahi et al., 2022; Themistocleous et al., 2020) | Eq. (3) |
| $NDMI = \frac{NIR - SWIR\,1}{NIR + SWIR\,1}$ | (Kikaki et al., 2022; Themistocleous et al., 2020) | Eq. (4) |
| $MNDWI = \frac{Green - SWIR\,2}{Green + SWIR\,2}$ | (Duarte and Azevedo, 2023; Themistocleous et al., 2020) | Eq. (5) |
| $SR = \frac{NIR}{Red}$ | (Themistocleous et al., 2020) | Eq. (6) |
| $RNDVI = \frac{RED - NDVI}{RED + NIR}$ | (Khetkeeree and Liangrocapart, 2021; Themistocleous et al., 2020) | Eq. (7) |
| $AWEI = (4\,x\,(Green - SWIR2) - (0.25\,x\,NIR + 2.75\,x\,SWIR1)$ | (Themistocleous et al., 2020) | Eq. (8) |
| $INDVI = \frac{0.9(RedEdge4) + 1.0(SWIR1) - 1.9(SWIR2) - 155}{1.1(RedEdge4) - 1.0(SWIR1) + 1.9(SWIR2) + 155}$ | (Khetkeeree and Liangrocapart, 2021) | Eq. (9) |
| $MINDVI = \frac{0.9(NIR) + 1.0(SWIR1) - 1.9(SWIR2) - 155}{1.1(NIR) - 1.0(SWIR1) + 1.9(SWIR2) + 155}$ | (Khetkeeree and Liangrocapart, 2021) | Eq. (10) |
| $PI = \frac{NIR}{NIR + Red}$ | (Gonzaga et al., 2021; Khetkeeree and Liangrocapart, 2021; Sannigrahi et al., 2022; Themistocleous et al., 2020) | Eq. (11) |
| $\mathbf{FDI} = \mathbf{NIR} - (\mathbf{RedEdge2}) + (\mathbf{SWIR1} - \mathbf{RedEdge2}) \times \frac{(\lambda_{NIR} - \lambda_{Red})}{(\lambda_{SWIR1} - \lambda_{Red})} \times \mathbf{10}$ | (Basu et al., 2021; Biermann et al., 2020; Duarte and Azevedo, 2023; Gonzaga et al., 2021; Hui et al., 2023; Jamali and Mahdianpari, 2021; Khetkeeree and Liangrocapart, 2021; Kikaki et al., 2022; Kremezi et al., 2022, 2021; Mifdal et al., 2021; Moshtaghi et al., 2021; Papageorgiou et al., 2022; Sannigrahi et al., 2022; Tasseron et al., 2021) | Eq. (12) |
| $\mathbf{HI} = (\lambda_B - \lambda_A) \times \frac{(R_C - R_A)}{(\lambda_C - \lambda_A)} + (R_A - R_B)$ | (Kremezi et al., 2021) (Kremezi et al., 2022) | Eq. (13) |
| $\mathbf{FAI} = NIR - Red - (SWIR1 - Red)\frac{(\lambda_{NIR} - \lambda_{Red})}{(\lambda_{SWIR1} - \lambda_{Red})}$ | (Kikaki et al., 2022; Kremezi et al., 2022) | Eq. (14) |
| $\mathbf{KNDVI} = tanh\,(NDVI)^2$ | (Sannigrahi et al., 2022) | Eq. (15) |
| $MARI = \frac{1}{Green} - \frac{1}{NIR}.NIR$ | (Duarte and Azevedo, 2023) | (Eq. 16) |

where $\lambda_{NIR}$, $\lambda_{Red}$, and $\lambda_{SWIR1}$ are the central wavelength of the band's NIR, Red, and SWIR1, respectively and RA; λA, RB; λB, and RC; λC are radiance/wavelength pairs for each index point.

## References


Abreo, N.A.S., Aurelio, R.M., Kobayashi, V.B., Thompson, K.F., 2023. 'Eye in the sky': off-the-shelf unmanned aerial vehicle (UAV) highlights exposure of marine turtles to floating litter (FML) in nearshore waters of Mayo Bay, Philippines. Mar. Pollut. Bull. 186, 114489 https://doi.org/10.1016/j.marpolbul.2022.114489.

Abreu, A., Pedrotti, M.L., 2019. Microplastics in the oceans: the solutions lie on land. F. Actions Sci. Reports. https://doi.org/10.1126/science.1260352.

Acuna-Ruz, T., Uribe, D., Taylor, R., Amezquita, L., Guzman, M.C., Merrill, J., Martinez, P., Voisin, L., Mattar, C., 2018. Anthropogenic marine debris over beaches: spectral characterization for remote sensing applications. Remote Sens. Environ. 217, 309–322. https://doi.org/10.1016/j.rse.2018.08.008.

Adam, I., Walker, T.R., Bezerra, J.C., Clayton, A., 2020. Policies to reduce single-use plastic marine pollution in West Africa. Mar. Policy 116, 103928. https://doi.org/10.1016/j.marpol.2020.103928.

Almeida, S., Radeta, M., Kataoka, T., Canning-Clode, J., Pessanha Pais, M., Freitas, R., Monteiro, J.G., 2023. Designing unmanned aerial survey monitoring program to assess floating litter contamination. Remote Sens. (Basel) 15. https://doi.org/10.3390/rs15010084.

Almroth, B.C., Eggert, H., 2019. Marine plastic pollution: sources, impacts, and policy issues. Rev. Environ. Econ. Policy 13, 317–326. https://doi.org/10.1093/reep/rez012.

Alosairi, Y., Al-Ragum, A., Al-Houti, D., 2021. Environmental mechanisms associated with fish kill in a semi-enclosed water body: an integrated numerical modeling approach. Ecotoxicol. Environ. Saf. 217, 112238 https://doi.org/10.1016/j.ecoenv.2021.112238.

Andriolo, U., Goncalves, G., Sobral, P., Fontan-Bouzas, A., Bessa, F., 2020. Beach-dune morphodynamics and marine macro-litter abundance: an integrated approach with unmanned aerial system. Sci. Total Environ. 749 https://doi.org/10.1016/j.scitotenv.2020.141474.

Aoki, Y., Arii, M., Koiwa, M., IEEE, 2013. Spaceborne SAR data analysis for marine debris after the Great East Japan Earthquake. In: Conf. Proc. 2013 ASIA-PACIFIC Conf. Synth. APERTURE RADAR.

Aoyama, T., 2016. Extraction of marine debris in the sea of Japan using high-spatial-resolution satellite images. In: Frouin, R.J., Shenoi, S.C., Rao, K.H. (Eds.), Remote Sensing of the Oceans and Inland Waters: Techniques, Applications, and Challenges. SPIE, pp. 213–219. https://doi.org/10.1117/12.2220370.

Arii, M., Aoki, Y., Koiwa, M., 2012. Effective monitoring for MARINE debris after Great East Japan Earthquake by using spaceborne synthetic aperture radar. Remote Sens. Mar. Environ. II https://doi.org/10.1117/12.975938.

Armitage, S., Awty-Carroll, K., Clewley, D., Martinez-Vicente, V., 2022. Detection and classification of floating plastic litter using a vessel-mounted video camera and deep learning. Remote Sens. (Basel) 14, 1–18. https://doi.org/10.3390/rs14143425.

Asadzadeh, S., de Souza Filho, C.R., 2016. Investigating the capability of WorldView-3 superspectral data for direct hydrocarbon detection. Remote Sens. Environ. 173, 162–173. https://doi.org/10.1016/j.rse.2015.11.030.

Balsi, M., Moroni, M., Chiarabini, V., Tanda, G., 2021. High-resolution aerial detection of marine plastic litter by hyperspectral sensing. Remote Sens. (Basel) 13. https://doi.org/10.3390/rs13081557.

Basu, B., Sannigrahi, S., Basu, A.S., Pilla, F., 2021. Development of novel classification algorithms for detection of floating plastic debris in coastal waterbodies using multispectral Sentinel-2 remote sensing imagery. Remote Sens. (Basel) 13. https://doi.org/10.3390/rs13081598.

Biermann, L., Clewley, D., Martinez-Vicente, V., Topouzelis, K., 2020. Finding plastic patches in coastal waters using optical satellite data. Sci. Rep. 10 https://doi.org/10.1038/s41598-020-62298-z.

Booth, H., Ma, W., Karakuş, O., 2023. High-precision density mapping of marine debris and floating plastics via satellite imagery. Sci. Rep. 13, 1–12. https://doi.org/10.1038/s41598-023-33612-2.

Borrelle, S.B., Ringma, J., Law, K.L., Monnahan, C.C., Lebreton, L., McGivern, A., Murphy, E., Jambeck, J., Leonard, G.H., Hilleary, M.A., Eriksen, M., Possingham, H.P., Rochman, C.M., 2020. Predicted growth in plastic waste exceeds efforts to mitigate plastic pollution. Science (80-. ) 1518, 1515–1518.

Bradney, L., Wijesekara, H., Palansooriya, K.N., Obadamudalige, N., Bolan, N.S., Ok, Y.S., Rinklebe, J., Kim, K.H., Kirkham, M.B., 2019. Particulate plastics as a vector for toxic trace-element uptake by aquatic and terrestrial organisms and human health risk. Environ. Int. 131 https://doi.org/10.1016/j.envint.2019.104937.

Brandon, J.A., Freibott, A., Sala, L.M., 2020. Patterns of suspended and salp-ingested microplastic debris in the North Pacific investigated with epifluorescence microscopy. Limnol. Oceanogr. Lett. 5, 46–53. https://doi.org/10.1002/lol2.10127.

Cecchi, T., 2021. Analysis of volatiles organic compounds in Venice lagoon water reveals COVID 19 lockdown impact on microplastics and mass tourism related pollutants. Sci. Total Environ. 783 https://doi.org/10.1016/j.scitotenv.2021.146951.

Chavez, P.S., 1988. An improved dark-object subtraction technique for atmospheric scattering correction of multispectral data. Remote Sens. Environ. https://doi.org/10.1016/0034-4257(88)90019-3.

Chitrakar, P., Baawain, M.S., Sana, A., Al-Mamun, A., 2019. Current status of marine pollution and mitigation strategies in arid region: a detailed review. Ocean Sci. J. 54, 317–348. https://doi.org/10.1007/s12601-019-0027-5.

Ciappa, A.C., 2022. Marine litter detection by Sentinel-2: a case study in north Adriatic (summer 2020). Remote Sens. (Basel) 14. https://doi.org/10.3390/rs14102409.

Cocking, J., Narayanaswamy, B.E., Waluda, C.M., Williamson, B.J., 2022. Aerial detection of beached marine plastic using a novel, hyperspectral short-wave infrared (SWIR) camera. ICES J. Mar. Sci. 79, 648–660. https://doi.org/10.1093/icesjms/fsac006.

Cole, M., Lindeque, P., Halsband, C., Galloway, T.S., 2011. Microplastics as contaminants in the marine environment: a review. Mar. Pollut. Bull. 62, 2588–2597. https://doi.org/10.1016/j.marpolbul.2011.09.025.

Cózar, A., Aliani, S., Basurko, O.C., Arias, M., Isobe, A., Topouzelis, K., Rubio, A., Morales-Caselles, C., Cozar, A., Aliani, S., Basurko, O.C., Arias, M., Isobe, A., Topouzelis, K., Rubio, A., Morales-Caselles, C., 2021. Marine litter windrows: a strategic target to understand and manage the ocean plastic pollution. Front. Mar. Sci. 8 https://doi.org/10.3389/fmars.2021.571796.

Dang, F., Wang, Q., Huang, Y., Wang, Y., Xing, B., 2022. Key knowledge gaps for one health approach to mitigate nanoplastic risks. Eco-Environ. Heal. 1, 11–22. https://doi.org/10.1016/j.eehl.2022.02.001.

Dasgupta, S., Sarraf, M., Wheeler, D., 2022. Plastic waste cleanup priorities to reduce marine pollution: a spatiotemporal analysis for Accra and Lagos with satellite data. Sci. Total Environ. 839, 156319 https://doi.org/10.1016/j.scitotenv.2022.156319.

Davaasuren, N., Marino, A., Boardman, C., Alparone, M., Nunziata, F., Ackermann, N., Hajnsek, I., IEEE, 2018. Detecting microplastics pollution in world oceans using sar remote sensing. In: IGARSS 2018–2018 IEEE Int. Geosci. Remote Sens. Symp.

de Vries, R., Egger, M., Mani, T., Lebreton, L., 2021. Quantifying floating plastic debris at sea using vessel-based optical data and artificial intelligence. Remote Sens. (Basel) 13. https://doi.org/10.3390/rs13173401.

Duarte, M.M., Azevedo, L., 2023. Automatic detection and identification of floating marine debris using multi-spectral satellite imagery. IEEE Trans. Geosci. Remote Sens. 61, 1–15. https://doi.org/10.1109/TGRS.2023.3283607.

El Mahrad, B., Newton, A., Icely, J.D., Kacimi, I., Abalansa, S., Snoussi, M., 2020. Contribution of remote sensing technologies to a holistic coastal and marine environmental management framework: a review. Remote Sens. (Basel) 12. https://doi.org/10.3390/rs12142313.

ESA, 2021. The discovery campaign on remote sensing of plastic marine litter [WWW Document]. URL. https://www.esa.int/Enabling_Support/Preparing_for_the_Future/Discovery_and_Preparation/The_Discovery_Campaign_on_Remote_Sensing_of_Plastic_Marine_Litter (accessed 9.10.23).

Farré, M., 2020. Remote and in situ devices for the assessment of marine contaminants of emerging concern and plastic debris detection. Curr. Opin. Environ. Sci. Heal. 18, 79–94. https://doi.org/10.1016/j.coesh.2020.10.002.

Feygels, V., Aitken, J., Ramnath, V., Duong, H., Marthouse, R., Smith, B., Clark, N., Renz, E., Reisser, J., Kopilevich, Y., IEEE, 2017. Coastal Zone Mapping and Imaging Lidar (CZMIL). In: Participation in the Ocean Cleanup's Aerial Expedition Project, in: OCEANS 2017 - ANCHORAGE. IEEE Explore, Anchorage, AK, USA.

Freitas, S., Silva, H., Silva, E., 2022. Hyperspectral imaging zero-shot learning for remote marine litter detection and classification. Remote Sens. (Basel) 14, 1–18. https://doi.org/10.3390/rs14215516.

Gall, S.C., Thompson, R.C., 2015. The impact of debris on marine life. Mar. Pollut. Bull. 92, 170–179. https://doi.org/10.1016/j.marpolbul.2014.12.041.

Garaba, S.P., Dierssen, H.M., 2018. An airborne remote sensing case study of synthetic hydrocarbon detection using short wave infrared absorption features identified from marine-harvested macro- and microplastics. Remote Sens. Environ. 205, 224–235. https://doi.org/10.1016/j.rse.2017.11.023.

Garaba, S.P., Dierssen, H.M., 2020. Hyperspectral ultraviolet to shortwave infrared characteristics of marine-harvested, washed-ashore and virgin plastics. Earth Syst. Sci. Data 12, 77–86. https://doi.org/10.5194/essd-12-77-2020.

Garaba, S.P., Aitken, J., Slat, B., Dierssen, H.M., Lebreton, L., Zielinski, O., Reisser, J., 2018. Sensing ocean plastics with an airborne hyperspectral shortwave infrared imager. Environ. Sci. Technol. 52, 11699–11707. https://doi.org/10.1021/acs.est.8b02855.

Garaba, S.P., Arias, M., Corradi, P., Harmel, T., de Vries, R., Lebreton, L., 2021. Concentration, anisotropic and apparent colour effects on optical reflectance properties of virgin and ocean-harvested plastics. J. Hazard. Mater. 406 https://doi.org/10.1016/j.jhazmat.2020.124290.

Garcia-Garin, O., Aguilar, A., Borrell, A., Gozalbes, P., Lobo, A., Penades-Suay, J., Raga, J.A., Revuelta, O., Serrano, M., Vighi, M., 2020a. Who's better at spotting? A comparison between aerial photography and observer-based methods to monitor floating marine litter and marine mega-fauna. Environ. Pollut. 258 https://doi.org/10.1016/j.envpol.2019.113680.

Garcia-Garin, O., Borrell, A., Aguilar, A., Cardona, L., Vighi, M., 2020b. Floating marine macro-litter in the North Western Mediterranean Sea: results from a combined monitoring approach. Mar. Pollut. Bull. 159 https://doi.org/10.1016/j.marpolbul.2020.111467.

Garcia-Garin, O., Monleon-Getino, T., Lopez-Brosa, P., Borrell, A., Aguilar, A., Borja-Robalino, R., Cardona, L., Vighi, M., 2021. Automatic detection and quantification of floating marine macro-litter in aerial images: introducing a novel deep learning approach connected to a web application in R. Environ. Pollut. 273 https://doi.org/10.1016/j.envpol.2021.116490.

Ge, Z.P., Shi, H.H., Mei, X.F., Dai, Z.J., Li, D.J., 2016. Semi-automatic recognition of marine debris on beaches. Sci. Rep. 6 https://doi.org/10.1038/srep25759.

Gnann, N., Baschek, B., Ternes, T.A., 2022. Close-range remote sensing-based detection and identification of macroplastics on water assisted by artificial intelligence: a review. Water Res. 222 https://doi.org/10.1016/j.watres.2022.118902.

Goddijn-Murphy, L., Dufaur, J., 2018. Proof of concept for a model of light reflectance of plastics floating on natural waters. Mar. Pollut. Bull. 135, 1145–1157. https://doi.org/10.1016/j.marpolbul.2018.08.044.

Goddijn-Murphy, L., Williamson, B., 2019. On thermal infrared remote sensing of plastic pollution in natural waters. Remote Sens. (Basel) 11. https://doi.org/10.3390/rs11182159.

Goddijn-Murphy, L., Williamson, B.J., McIlvenny, J., Corradi, P., 2022. Using a UAV thermal infrared camera for monitoring floating marine plastic litter. Remote Sens. (Basel) 14, 1–25. https://doi.org/10.3390/rs14133179.

Goncalves, G., Andriolo, U., Pinto, L., Bessa, F., 2020. Mapping marine litter using UAS on a beach-dune system: a multidisciplinary approach. Sci. Total Environ. 706 https://doi.org/10.1016/j.scitotenv.2019.135742.

Gong, W.W., Xing, Y., Han, L.H., Lu, A.X., Qu, H., Xu, L., 2022. Occurrence and distribution of micro- and mesoplastics in the high-latitude nature reserve, northern China. Front. Environ. Sci. Eng. 16 https://doi.org/10.1007/s11783-022-1534-7.

Gonzaga, M.L.R., Wong, M.T.S., Blanco, A.C., Principe, J.A., 2021. Utilization of sentinel-2 imagery in the estimation of plastics among floating debris along the coast of manila bay. In: International Archivees of the Photogrammetry, Remote Sensing and Spatial Information Sciences - ISPRS Archives, pp. 177–184. https://doi.org/10.5194/isprs-Archives-XLVI-4-W6-2021-177-2021.

Guffogg, J.A., Blades, S.M., Soto-Berelov, M., Bellman, C.J., Skidmore, A.K., Jones, S.D., 2021. Quantifying marine plastic debris in a beach environment using spectral analysis. Remote Sens. (Basel) 13. https://doi.org/10.3390/rs13224548.

Guo, X., Li, P., 2020. Mapping plastic materials in an urban area: development of the normalized difference plastic index using WorldView-3 superspectral data. ISPRS J. Photogramm. Remote Sens. 169, 214–226. https://doi.org/10.1016/j.isprsjprs.2020.09.009.

Hanvey, J.S., Lewis, P.J., Lavers, J.L., Crosbie, N.D., Pozo, K., Clarke, B.O., 2017. A review of analytical techniques for quantifying microplastics in sediments. Anal. Methods 9, 1369–1383. https://doi.org/10.1039/c6ay02707e.

Hu, C., 2009. A novel ocean color index to detect floating algae in the global oceans. Remote Sens. Environ. 113, 2118–2129. https://doi.org/10.1016/j.rse.2009.05.012.

Hu, C.M., 2021. Remote detection of marine debris using satellite observations in the visible and near infrared spectral range: challenges and potentials. Remote Sens. Environ. 259 https://doi.org/10.1016/j.rse.2021.112414.

Hu, C., 2022. Remote detection of marine debris using Sentinel-2 imagery: a cautious note on spectral interpretations. Mar. Pollut. Bull. 183, 114082 https://doi.org/10.1016/j.marpolbul.2022.114082.

Hu, C., Qi, L., Xie, Y., Zhang, S., Barnes, B.B., 2022. Spectral characteristics of sea snot reflectance observed from satellites: implications for remote sensing of marine debris. Remote Sens. Environ. 269 https://doi.org/10.1016/j.rse.2021.112842.

Hu, C., Qi, L., Wang, M., Park, Y.-J., 2023. Floating debris in the northern Gulf of Mexico after hurricane Katrina. Environ. Sci. Technol. https://doi.org/10.1021/acs.est.3c01689.

Hueni, A., Bertschi, S., 2020. Detection of sub-pixel plastic abundance on water surfaces using airborne imaging spectroscopy. In: IGARSS 2020–2020 IEEE Int. Geosci. Remote Sens. Symp. IEEE. https://doi.org/10.1109/IGARSS39084.2020.9323556.

Hui, J., Sato, T., Kanao, S., 2023. Numerical estimation of the hotspot positions of floating plastic debris in the Tsushima Strait using the adjoint marginal sensitivity method. Ocean Eng. 270, 113606 https://doi.org/10.1016/j.oceaneng.2022.113606.

Jamali, A., Mahdianpari, M., 2021. A cloud-based framework for large-scale monitoring of ocean plastics using multi-spectral satellite imagery and generative adversarial network. Water 13. https://doi.org/10.3390/w13182553.

Jambeck, J.R., Geyer, R., Wilcox, C., Siegler, T.R., Perryman, M., Andrady, A., Narayan, R., Law, K.L., 2015. Plastic waste inputs from land into the ocean. Science (80-. ) 347, 768–771. https://doi.org/10.1126/science.1260352.

Kanhai, L.D.K., Asmath, H., Gobin, J.F., 2022. The status of marine debris/litter and plastic pollution in the Caribbean large marine ecosystem (CLME): 1980–2020. Environ. Pollut. 300, 118919 https://doi.org/10.1016/j.envpol.2022.118919.

Khetkeeree, S., Liangrocapart, S., 2021. Detecting floating plastic marine debris using sentinel-2 data via modified infrared NDVI. In: ECTI-CON 2021–2021 18th International Conference on Electrical Engineering/Electronics, Computer, Telecommunications and Information Technology: Smart Electrical System and Technology, Proceedings, pp. 633–636. https://doi.org/10.1109/ECTI-CON51831.2021.9454748.

Kikaki, A., Karantzalos, K., Power, C.A., Raitsos, D.E., 2020. Remotely sensing the source and transport of marine plastic debris in Bay Islands of Honduras (Caribbean Sea). Remote Sens. (Basel) 12. https://doi.org/10.3390/rs12111727.

Kikaki, K., Kakogeorgiou, I., Mikeli, P., Raitsos, D.E., Karantzalos, K., 2022. MARIDA: a benchmark for marine debris detection from Sentinel-2 remote sensing data. PloS One 17. https://doi.org/10.1371/journal.pone.0262247.

Kremezi, M., Kristollari, V., Karathanassi, V., Topouzelis, K., Kolokoussis, P., Taggio, N., Aiello, A., Ceriola, G., Barbone, E., Corradi, P., 2021. Pansharpening PRISMA data for marine plastic litter detection using plastic indexes. IEEE ACCESS 9, 61955–61971. https://doi.org/10.1109/ACCESS.2021.3073903.

Kremezi, M., Kristollari, V., Karathanassi, V., Topouzelis, K., Kolokoussis, P., Taggio, N., Aiello, A., Ceriola, G., Barbone, E., Corradi, P., 2022. Increasing the Sentinel-2 potential for marine plastic litter monitoring through image fusion techniques. Mar. Pollut. Bull. 182 https://doi.org/10.1016/j.marpolbul.2022.113974.

Kruse, C., Boyda, E., Chen, S., Karra, K., Bou-Nahra, T., Hammer, D., Mathis, J., Maddalene, T., Jambeck, J., Laurier, F., 2023. Satellite monitoring of terrestrial plastic waste. PloS One 18, 1–20. https://doi.org/10.1371/journal.pone.0278997.

Kühn, F., Oppermann, K., Hörig, B., 2004. Hydrocarbon index - an algorithm for hyperspectral detection of hydrocarbons. Int. J. Remote Sens. 25, 2467–2473. https://doi.org/10.1080/01431160310001642287.

Lanorte, A., De Santis, F., Nolè, G., Blanco, I., Loisi, R.V., Schettini, E., Vox, G., 2017. Agricultural plastic waste spatial estimation by Landsat 8 satellite images. Comput. Electron. Agric. 141, 35–45. https://doi.org/10.1016/j.compag.2017.07.003.

Law, K.L., Morét-Ferguson, S., Maximenko, N.A., Proskurowski, G., Peacock, E.E., Hafner, J., Reddy, C.M., 2010. Plastic accumulation in the North Atlantic subtropical gyre. Science (80-. ) 329, 1185–1188. https://doi.org/10.1126/science.1192321.

Lebreton, L.C.M., Van Der Zwet, J., Damsteeg, J.W., Slat, B., Andrady, A., Reisser, J., 2017. River plastic emissions to the world's oceans. Nat. Commun. 8, 1–10. https://doi.org/10.1038/ncomms15611.

Lebreton, L., Slat, B., Ferrari, F., Sainte-Rose, B., Aitken, J., Marthouse, R., Hajbane, S., Cunsolo, S., Schwarz, A., Levivier, A., Noble, K., Debeljak, P., Maral, H., Schoeneich-Argent, R., Brambini, R., Reisser, J., 2018. Evidence that the great Pacific garbage patch is rapidly accumulating plastic. Sci. Rep. 8 https://doi.org/10.1038/s41598-018-22939-w.

Lins-Silva, N., Marcolin, C.R., Kessler, F., Schwamborn, R., 2021. A fresh look at microplastics and other particles in the tropical coastal ecosystems of Tamandare, Brazil. Mar. Environ. Res. 169 https://doi.org/10.1016/j.marenvres.2021.105327.

Livens, S., Knaeps, E., Dries, J., 2022. Feasibility Assessment of a Dedicated Satellite Mission for Monitoring Marine Macroplastics.

Mace, T.H., 2012. At-sea detection of marine debris: overview of technologies, processes, issues, and options. Mar. Pollut. Bull. 65, 23–27. https://doi.org/10.1016/j.marpolbul.2011.08.042.

Marshall, M., 2018. From pollution to solution. In: New Scientist. https://doi.org/10.1016/S0262-4079(18)30486-X.

Martínez-Vicente, V., Clark, J.R., Corradi, P., Aliani, S., Arias, M., Bochow, M., Bonnery, G., Cole, M., Cózar, A., Donnelly, R., Echevarría, F., Galgani, F., Garaba, S. P., Goddijn-Murphy, L., Lebreton, L., Leslie, H.A., Lindeque, P.K., Maximenko, N., Martin-Lauzer, F.-R., Moller, D., Murphy, P., Palombi, L., Raimondi, V., Reisser, J., Romero, L., Simis, S.G.H., Sterckx, S., Thompson, R.C., Topouzelis, K.N., van Sebille, E., Veiga, J.M., Vethaak, A.D., 2019. Measuring marine plastic debris from space: initial assessment of observation requirements. Remote Sens. (Basel) 11. https://doi.org/10.3390/rs11202443.

Maximenko, Nikolai, Corradi, P., Law, K.L., Van Sebille, E., Garaba, S.P., Lampitt, R.S., Galgani, F., Martinez-Vicente, V., Goddijn-Murphy, L., Veiga, J.M., Thompson, R.C., Maes, C., Moller, D., Löscher, C.R., Addamo, A.M., Lamson, M., Centurioni, L.R., Posth, N., Lumpkin, R., Vinci, M., Martins, A.M., Pieper, C.D., Isobe, A., Hanke, G., Edwards, M., Chubarenko, I.P., Rodriguez, E., Aliani, S., Arias, M., Asner, G.P., Brosich, A., Carlton, J.T., Chao, Y., Cook, A.M., Cundy, A., Galloway, T.S., Giorgetti, A., Goni, G.J., Guichoux, Y., Hardesty, B.D., Holdsworth, N., Lebreton, L., Leslie, H.A., Macadam-Somer, I., Mace, T., Manuel, M., Marsh, R., Martinez, E., Mayor, D., Le Moigne, M., Jack, M.E.M., Mowlem, M.C., Obbard, R.W., Pabortsava, K., Robberson, B., Rotaru, A.E., Spedicato, M.T., Thiel, M., Turra, A., Wilcox, C., 2019. Towards the integrated marine debris observing system. Front. Mar. Sci. 6 https://doi.org/10.3389/fmars.2019.00447.

Mehrubeoglu, M., Van Sickle, A., Turner, J., 2020. Detection and Identification of Plastics Using SWIR Hyperspectral Imaging. XXIV Appl. SENSORS, Process, IMAGING Spectrom. https://doi.org/10.1117/12.2570040.

Meijer, L.J.J., van Emmerik, T., van der Ent, R., Schmidt, C., Lebreton, L., 2021. More than 1000 rivers account for 80\% of global riverine plastic emissions into the ocean. Sci. Adv. 7, eaaz5803. https://doi.org/10.1126/sciadv.aaz5803.

Mifdal, J., Longepe, N., Rußwurm, M., 2021. Towards detecting floating objects on a global scale with learned spatial features using sentinel 2. In: ISPRS Annals of the Photogrammetry, Remote Sensing and Spatial Information Sciences, pp. 285–293. https://doi.org/10.5194/isprs-annals-V-3-2021-285-2021.

Moshtaghi, M., Knaeps, E., Sterckx, S., Garaba, S., Meire, D., 2021. Spectral reflectance of marine macroplastics in the VNIR and SWIR measured in a controlled environment. Sci. Rep. 11 https://doi.org/10.1038/s41598-021-84867-6.

Mouat, J., Lopez Lozano, R., Bateson, H., 2010. Economic Impacts of Marine Litter. Kommunernes Internationale Miljoorganisation, KMO.

Mukonza, S.S., Chiang, J.-L., 2022. Satellite sensors as an emerging technique for monitoring macro- and microplastics in aquatic ecosystems. Water Emerg. Contam. Nanoplastics 1, 17. https://doi.org/10.20517/wecn.2022.12.

Nagy, M., Istrate, L., Simtinică, M., Travadel, S., Blanc, P., 2022. Automatic detection of marine litter: a general framework to leverage synthetic data. Remote Sens. (Basel) 14, 1–21. https://doi.org/10.3390/rs14236102.

Nakajima, R., Miyama, T., Kitahashi, T., Isobe, N., Nagano, Y., Ikuta, T., Oguri, K., Tsuchiya, M., Yoshida, T., Aoki, K., Maeda, Y., Kawamura, K., Suzukawa, M., Yamauchi, T., Ritchie, H., Fujikura, K., Yabuki, A., 2022. Plastic after an extreme storm: the typhoon-induced response of micro- and mesoplastics in coastal waters. Front. Mar. Sci. 8, 1–11. https://doi.org/10.3389/fmars.2021.806952.

NASA, 2022. Research Opportunities in Space and Earth Sciences (ROSES) [WWW Document]. URL. https://science.nasa.gov/researchers/solicitations/roses-2022/research-opportunities-space-and-earth-sciences-roses-2022-be-released-february-14-2022.

Novelli, A., Tarantino, E., 2015. The contribution of Landsat 8 TIRS sensor data to the identification of plastic covered vineyards. In: Hadjimitsis, D.G., Themistocleous, K., Michaelides, S., Papadavid, G. (Eds.), Third International Conference on Remote Sensing and Geoinformation of the Environment (RSCy2015). SPIE, pp. 441–449. https://doi.org/10.1117/12.2192095.

OHHLEP, Adisasmito, W.B., Almuhairi, S., Behravesh, C.B., Bilivogui, P., Bukachi, S.A., Casas, N., Becerra, N.C., Charron, D.F., Chaudhary, A., Ciacci Zanella, J.R., Cunningham, A.A., Dar, O., Debnath, N., Dungu, B., Farag, E., Gao, G.F., Hayman, D. T.S., Khaitsa, M., Koopmans, M.P.G., Machalaba, C., Mackenzie, J.S., Markotter, W., Mettenleiter, T.C., Morand, S., Smolenskiy, V., Zhou, L., 2022. One health: a new definition for a sustainable and healthy future. PLoS Pathog. 18, 2020–2023. https://doi.org/10.1371/journal.ppat.1010537.

Olyaei, M., Ebtehaj, A., Hong, J., 2022. Optical detection of marine debris using deep knockoff. IEEE Trans. Geosci. Remote Sens. 60, 1–12. https://doi.org/10.1109/TGRS.2022.3228638.

Omali, T.U., 2018. Impacts of sensor spatial resolution on remote sensing image classification. Glob. Sci. 6, 23–35.

Ormaza-Gonzaìlez, F.I., Castro-Rodas, D., Statham, P.J., Ormaza-Gonzalez, F.I., Castro-Rodas, D., Statham, P.J., 2021. COVID-19 impacts on beaches and coastal water pollution at selected sites in Ecuador, and management proposals post-pandemic. Front. Mar. Sci. 8 https://doi.org/10.3389/fmars.2021.669374.

Page, R., Lavender, S., Thomas, D., Berry, K., Stevens, S., Haq, M., Udugbezi, E., Fowler, G., Best, J., Brockie, I., 2020. Identification of Tyre and plastic waste from combined copernicus sentinel-1 and-2 data. Remote Sens. (Basel) 12, 1–14. https://doi.org/10.3390/rs12172824.

Papageorgiou, D., Topouzelis, K., Suaria, G., Aliani, S., Corradi, P., 2022. Sentinel-2 detection of floating marine litter targets with partial spectral unmixing and spectral comparison with other floating materials (plastic litter project 2021). Remote Sens. (Basel) 14. https://doi.org/10.3390/rs14235997.

Park, Y.J., Garaba, S.P., Sainte-Rose, B., 2021. Detecting the great Pacific garbage patch floating plastic litter using WorldView-3 satellite imagery. Opt. Express 29, 35288–35298. https://doi.org/10.1364/OE.440380.

Peng, L., Fu, D., Qi, H., Lan, C.Q., Yu, H., Ge, C., 2020. Micro- and nano-plastics in marine environment: source, distribution and threats — a review. Sci. Total Environ. 698, 134254 https://doi.org/10.1016/j.scitotenv.2019.134254.

Phelan, A.A., Ross, H., Setianto, N.A., Fielding, K., Pradipta, L., 2020. Ocean plastic crisis-mental models of plastic pollution from remote Indonesian coastal communities. PloS One 15, e0236149. https://doi.org/10.1371/journal.pone.0236149.

Phillips, W., Thorne, E., Roopnarine, C., 2020. Economic Implications of the Ban on Plastics in the Caribbean: A Case Study of Trinidad and Tobago, Studies and Perspectives Series-ECLAC Subregional Headquarters for the Caribbean, No. 95 (LC/TS.2020/127-LC/CAR/TS.2020/5), Santiago, Economic Commission for Latin America and the Caribbean (ECLAC)..

Pichel, W.G., Veenstra, T.S., Churnside, J.H., Arabini, E., Friedman, K.S., Foley, D.G., Brainard, R.E., Kiefer, D., Ogle, S., Clemente-Colón, P., Li, X., 2012. GhostNet marine debris survey in the Gulf of Alaska - satellite guidance and aircraft observations. Mar. Pollut. Bull. 65, 28–41. https://doi.org/10.1016/j.marpolbul.2011.10.009.

PLP, 2023. Plastic Litter Project [WWW Document]. URL. http://plp.aegean.gr/category/experiment-log-2023/.

Prata, J.C., Silva, A.L.P., da Costa, J.P., Mouneyrac, C., Walker, T.R., Duarte, A.C., Rocha-Santos, T., 2019. Solutions and integrated strategies for the control and mitigation of plastic and microplastic pollution. Int. J. Environ. Res. Public Health 16. https://doi.org/10.3390/ijerph16132411.

Rakib, M.R.J., De-la-Torre, G.E., Pizarro-Ortega, C.I., Dioses-Salinas, D.C., Al-Nahian, S., 2021. Personal protective equipment (PPE) pollution driven by the COVID-19 pandemic in Cox's Bazar, the longest natural beach in the world. Mar. Pollut. Bull. 169 https://doi.org/10.1016/j.marpolbul.2021.112497.

Ramavaram, H.R., Kotichintala, S., Naik, S., Critchley-Marrows, J., Isaiah, O.T., Pittala, M., Wan, S., Irorere, D., 2018. Tracking ocean plastics using aerial and space borne platforms: overview of techniques and challenges. In: Proceedings of the International Astronautical Congress, IAC.

Sakti, A.D., Rinasti, A.N., Agustina, E., Diastomo, H., Muhammad, F., Anna, Z., Wikantika, K., 2021. Multi-scenario model of plastic waste accumulation potential in Indonesia using integrated remote sensing, statistic and socio-demographic data. ISPRS Int. J. Geo-Inf. 10 https://doi.org/10.3390/ijgi10070481.

Salgado-Hernanz, P.M., Bauza, J., Alomar, C., Compa, M., Romero, L., Deudero, S., 2021. Assessment of marine litter through remote sensing: recent approaches and future goals. Mar. Pollut. Bull. 168 https://doi.org/10.1016/j.marpolbul.2021.112347.

Sannigrahi, S., Basu, B., Basu, A.S., Pilla, F., 2022. Development of automated marine floating plastic detection system using Sentinel-2 imagery and machine learning models. Mar. Pollut. Bull. 178, 113527 https://doi.org/10.1016/j.marpolbul.2022.113527.

Sasaki, K., Sekine, T., Burtz, L.J., Emery, W.J., 2022. Coastal marine debris detection and density mapping with very high resolution satellite imagery. IEEE J. Sel. Top. Appl. Earth Obs. Remote Sens. 15, 6391–6401. https://doi.org/10.1109/JSTARS.2022.3193993.

Savastano, S., Cester, I., Perpinyá, M., Romero, L., 2021. A first approach to the automatic detection of marine litter in sar images using artificial intelligence. In: Int. Geosci. Remote Sens. Symp. 2021-Janua, pp. 8704–8707. https://doi.org/10.1109/IGARSS47720.2021.9737038.

Schmaltz, E., Melvin, E.C., Diana, Z., Gunady, E.F., Rittschof, D., Somarelli, J.A., Virdin, J., Dunphy-Daly, M.M., 2020. Plastic pollution solutions: emerging technologies to prevent and collect marine plastic pollution. Environ. Int. 144 https://doi.org/10.1016/j.envint.2020.106067.

Schmid, C., Cozzarini, L., Zambello, E., 2021. A critical review on marine litter in the Adriatic Sea: focus on plastic pollution. Environ. Pollut. 273, 116430 https://doi.org/10.1016/j.envpol.2021.116430.

Schmidt, L.K., Bochow, M., Imhof, H.K., Oswald, S.E., 2018. Multi-temporal surveys for microplastic particles enabled by a novel and fast application of SWIR imaging spectroscopy - study of an urban watercourse traversing the city of Berlin, Germany. Environ. Pollut. 239, 579–589. https://doi.org/10.1016/j.envpol.2018.03.097.

Schuyler, Q.A., Wilcox, C., Townsend, K.A., Wedemeyer-Strombel, K.R., Balazs, G., van Sebille, E., Hardesty, B.D., 2016. Risk analysis reveals global hotspots for marine debris ingestion by sea turtles. Glob. Chang. Biol. 22, 567–576. https://doi.org/10.1111/gcb.13078.

Sebille, E.V., Aliani, S., Law, K.L., Maximenko, N., Alsina, J.M., Bagaev, A., Bergmann, M., Chapron, B., Chubarenko, I., Cózar, A., Delandmeter, P., Egger, M., Fox-Kemper, B., Garaba, S.P., Goddijn-Murphy, L., Hardesty, B.D., Hoffman, M.J., Isobe, A., Jongedijk, C.E., Kaandorp, M.L.A., Khatmullina, L., Koelmans, A.A., Kukulka, T., Laufkötter, C., Lebreton, L., Lobelle, D., Maes, C., Martinez-Vicente, V.,

Morales Maqueda, M.A., Poulain-Zarcos, M., Rodríguez, E., Ryan, P.G., Shanks, A.L., Shim, W.J., Suaria, G., Thiel, M., Van Den Bremer, T.S., Wichmann, D., 2020. The physical oceanography of the transport of floating marine debris. Environ. Res. Lett. 15 https://doi.org/10.1088/1748-9326/ab6d7d.

Serafino, F., Bianco, A., 2021. Use of X-band radars to monitor small Garbage Islands. Remote Sens. (Basel) 13. https://doi.org/10.3390/rs13183558.

Serranti, S., Fiore, L., Bonifazi, G., Takeshima, A., Takeuchi, H., Kashiwada, S., 2019. Microplastics characterization by hyperspectral imaging in the SWIR range. In: SPIE Futur. Sens. Technol. https://doi.org/10.1117/12.2542793.

Simpson, M., Marino, A., De Maagt, P., Gandini, E., Hunter, P., Spyrakos, E., Tyler, A., 2022. Monitoring of large plastic accumulations near dams using sentinel-1 polarimetric sar data. In: Int. Geosci. Remote Sens. Symp. 2022-July, pp. 1504–1507. https://doi.org/10.1109/IGARSS46834.2022.9884484.

Simpson, M.D., Marino, A., de Maagt, P., Gandini, E., de Fockert, A., Hunter, P., Spyrakos, E., Telfer, T., Tyler, A., 2023. Investigating the backscatter of marine plastic litter using a C- and X-band ground radar, during a measurement campaign in Deltares. Remote Sens. (Basel) 15. https://doi.org/10.3390/rs15061654.

Sobhytta, E.Y., Astuti, R.Y., Dwiatmoko, R., Yudiarso, P., 2020. Mapping coastal marine debris flow using trajectory particle 2d modelling and aerial imagery (case study: tukad loloan and mertasari beach – bali). In: ACRS 2020 - 41st Asian Conference on Remote Sensing.

Sojobi, A.O., Zayed, T., 2022. Impact of sewer overflow on public health: a comprehensive scientometric analysis and systematic review. Environ. Res. 203, 111609 https://doi.org/10.1016/j.envres.2021.111609.

Taddia, Y., Corbau, C., Buoninsegni, J., Simeoni, U., Pellegrinelli, A., 2021. UAV approach for detecting plastic marine debris on the beach: a case study in the Po River Delta (Italy). DRONES 5. https://doi.org/10.3390/drones5040140.

Taggio, N., Aiello, A., Ceriola, G., Kremezi, M., Kristollari, V., Kolokoussis, P., Karathanassi, V., Barbone, E., 2022. A combination of machine learning algorithms for marine plastic litter detection exploiting hyperspectral PRISMA data. Remote Sens. (Basel) 14. https://doi.org/10.3390/rs14153606.

Tasseron, P., van Emmerik, T., Peller, J., Schreyers, L., Biermann, L., 2021. Advancing floating macroplastic detection from space using experimental hyperspectral imagery. Remote Sens. (Basel) 13. https://doi.org/10.3390/rs13122335.

Teng, C., Kylili, K., Hadjistassou, C., 2022. Deploying deep learning to estimate the abundance of marine debris from video footage. Mar. Pollut. Bull. 183, 114049 https://doi.org/10.1016/j.marpolbul.2022.114049.

The Ocean Cleanup, 2023. The ocean cleanup [WWW document]. URL. https://theoceancleanup.com/.

Themistocleous, K., Papoutsa, C., Michaelides, S., Hadjimitsis, D., 2020. Investigating detection of floating plastic litter from space using Sentinel-2 imagery. Remote Sens. (Basel) 12. https://doi.org/10.3390/rs12162648.

Thompson, R.C., Olson, Y., Mitchell, R.P., Davis, A., Rowland, S.J., John, A.W.G., McGonigle, D., Russell, A.E., 2004. Lost at sea: where is all the plastic? Science (80-.) 304, 838. https://doi.org/10.1126/science.1094559.

Topouzelis, K., Papakonstantinou, A., Garaba, S.P., 2019. Detection of floating plastics from satellite and unmanned aerial systems (plastic litter project 2018). Int. J. Appl. Earth Obs. Geoinf. 79, 175–183. https://doi.org/10.1016/j.jag.2019.03.011.

Topouzelis, K., Papageorgiou, D., Karagaitanakis, A., Papakonstantinou, A., Ballesteros, M.A., 2020a. Remote sensing of sea surface artificial floating plastic targets with Sentinel-2 and unmanned aerial systems (plastic litter project 2019). Remote Sens. (Basel) 12. https://doi.org/10.3390/rs12122013.

Topouzelis, K., Papageorgiou, D., Karagaitanakis, A., Papakonstantinou, A., Ballesteros, M.A., 2020b. Plastic litter project 2019: exploring the detection of floating plastic litter using drones and sentinel 2 satellite images. In: IGARSS 2020–2020 IEEE Int. Geosci. Remote Sens. Symp. IEEE. https://doi.org/10.1109/IGARSS39084.2020.9324548.

Topouzelis, K., Papageorgiou, D., Suaria, G., Aliani, S., 2021. Floating marine litter detection algorithms and techniques using optical remote sensing data: a review. Mar. Pollut. Bull. 170 https://doi.org/10.1016/j.marpolbul.2021.112675.

Tucker, C.J., 1979. Red and photographic infrared linear combinations for monitoring vegetation. Remote Sens. Environ. 8, 127–150. https://doi.org/10.1016/0034-4257(79)90013-0.

UN, 2016. Sustainable Development Goals [WWW Document].. United Nations. URL. https://www.un.org/sustainabledevelopment/sustainable-development-goals/.

Veenstra, T.S., Churnside, J.H., 2012. Airborne sensors for detecting large marine debris at sea. Mar. Pollut. Bull. 65, 63–68. https://doi.org/10.1016/j.marpolbul.2010.11.018.

Veettil, B.K., Hong Quan, N., Hauser, L.T., Doan Van, D., Quang, N.X., 2022. Coastal and marine plastic litter monitoring using remote sensing: a review. Estuar. Coast. Shelf Sci. 279, 108160 https://doi.org/10.1016/j.ecss.2022.108160.

Verstraete, M.M., Diner, D.J., Bézy, J.-L., 2015. Planning for a spaceborne earth observation mission: from user expectations to measurement requirements. Environ. Sci. Policy 54, 419–427. https://doi.org/10.1016/j.envsci.2015.08.005.

Vighi, M., Ruiz-Orejón, L.F., Hanke, G., European Commission. Joint Research Centre, 2022. MSFD technical group on marine litter. In: Monitoring of Floating Marine Macro Litter : State of the Art and Literature Overview. https://doi.org/10.2760/78914.

Viool, V., Gupta, A., Petten, L., Schalekamp, J., 2019. The price tag of plastic pollution - an economic assessment of river plastic. Deloitte 1–16 doi. https://www2.deloitte.com/content/dam/Deloitte/nl/Documents/strategy-analytics-and-ma/deloitte-nl-strategy-analytics-and-ma-the-price-tag-of-plastic-pollution.pdf.

Vitale, S., Ferraioli, G., Ali, M., Pascazio, V., Ricciotti, L., Roviello, G., Schirinzi, G., 2022. Marine plastic detection using optical data. In: Int. Geosci. Remote Sens. Symp. 2022-July, pp. 2662–2665. https://doi.org/10.1109/IGARSS46834.2022.9884610.

Walker, T.R., Grant, J., Archambault, M.C., 2006. Accumulation of marine debris on an intertidal beach in an urban park (Halifax Harbour, Nova Scotia). Water Qual. Res. J. Canada 41, 256–262. https://doi.org/10.2166/wqrj.2006.029.

Waqas, M., Nazeer, M., Shahzad, M., Zia, I., 2019. Spatial and temporal variability of Open-Ocean Barrier Islands along the Indus Delta region. Remote Sens. (Basel) 11, 437. https://doi.org/10.3390/rs11040437.

Wilcox, C., Van Sebille, E., Hardesty, B.D., 2015. Threat of plastic pollution to seabirds is global, pervasive, and increasing. Proc. Natl. Acad. Sci. 112, 11899–11904. https://doi.org/10.1073/pnas.1502108112.

Wolf, M., van den Berg, K., Garaba, S.P., Gnann, N., Sattler, K., Stahl, F., Zielinski, O., 2020. Machine learning for aquatic plastic litter detection, classification and quantification (APLASTIC-Q). Environ. Res. Lett. 15 https://doi.org/10.1088/1748-9326/abbd01.

Woodall, L.C., Sanchez-Vidal, A., Canals, M., Paterson, G.L.J., Coppock, R., Sleight, V., Calafat, A., Rogers, A.D., Narayanaswamy, B.E., Thompson, R.C., 2014. The deep sea is a major sink for microplastic debris. R. Soc. Open Sci. 1, 140317 https://doi.org/10.1098/rsos.140317.

Worm, B., Lotze, H.K., Jubinville, I., Wilcox, C., Jambeck, J., 2017. Plastic as a persistent marine pollutant. Annu. Rev. Env. Resour. 42, 1–26. https://doi.org/10.1146/annurev-environ-102016-060700.

Xanthos, D., Walker, T.R., 2017. International policies to reduce plastic marine pollution from single-use plastics (plastic bags and microbeads): a review. Mar. Pollut. Bull. 118, 17–26. https://doi.org/10.1016/j.marpolbul.2017.02.048.

Yuan, S., Li, Y., Bao, F., Xu, H., Yang, Y., Yan, Q., Zhong, S., Yin, H., Xu, J., Huang, Z., Lin, J., 2023. Marine environmental monitoring with unmanned vehicle platforms: present applications and future prospects. Sci. Total Environ. 858, 159741 https://doi.org/10.1016/j.scitotenv.2022.159741.

Yuying, H., Zhenpeng, G., Daoji, L., Huahong, S., Zhen, H., Zhijun, D., 2019. LiDAR-based quickly recognition of beach debris. Haiyang Xuebao 41, 156–162. https://doi.org/10.3969/j.issn.0253-4193.2019.11.015.

Zhang, D.D., Liu, X.D., Huang, W., Li, J.J., Wang, C.S., Zhang, D.S., Zhang, C.F., 2020. Microplastic pollution in deep-sea sediments and organisms of the Western Pacific Ocean. Environ. Pollut. 259 https://doi.org/10.1016/j.envpol.2020.113948.

Zhang, P., Du, P., Guo, S., Zhang, W., Tang, P., Chen, J., Zheng, H., 2022. A novel index for robust and large-scale mapping of plastic greenhouse from Sentinel-2 images. Remote Sens. Environ. 276, 113042 https://doi.org/10.1016/j.rse.2022.113042.